



**Division of Physical Chemistry, Institute of
Advanced Materials, Physicochemical Processes,
Nanotechnology and Microsystems,
Athens, Greece**

Efficiency and stability issues in dye sensitized solar cells

Polycarpos Falaras

Outline

Short introduction to DSCs

Results at NCSRD: State-of-the-art materials and devices (optimization)

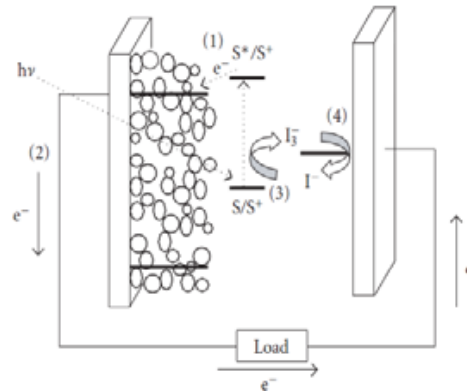
Stability issues/Scale-up/applications-commercialization

Towards new generation solar cells (perovskites)

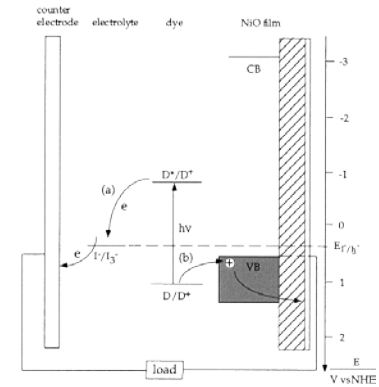
Next generation (3rd) PVs-Single junction solar cells

DSCs
 Organic Photovoltaics (OPVs):
 QDSCs
 Nanocrystal-based solar cells

PSCs
 SMSCs



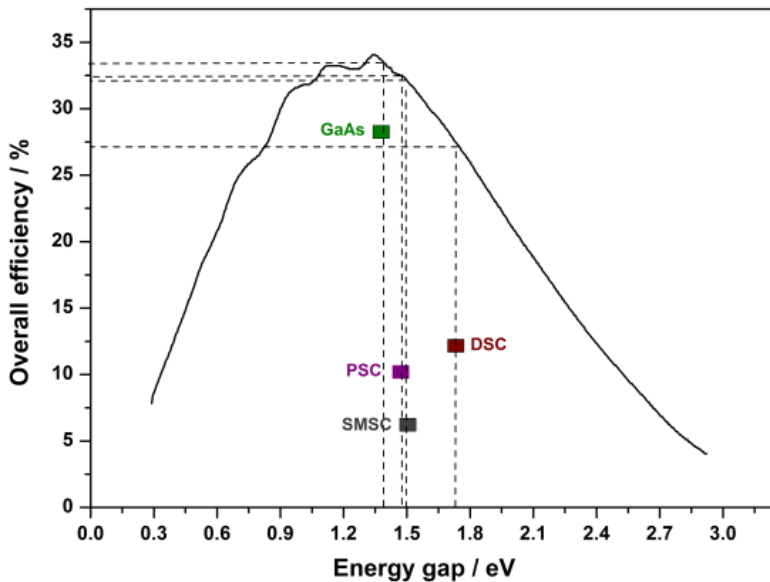
n-type DSC



p-type DSC

n-type DSCs

optical gap 1.73 eV
 (J_{sc}/J_{max}) 82%
 V_{oc}/V_{max} 67%
 TiO₂ low conductivity

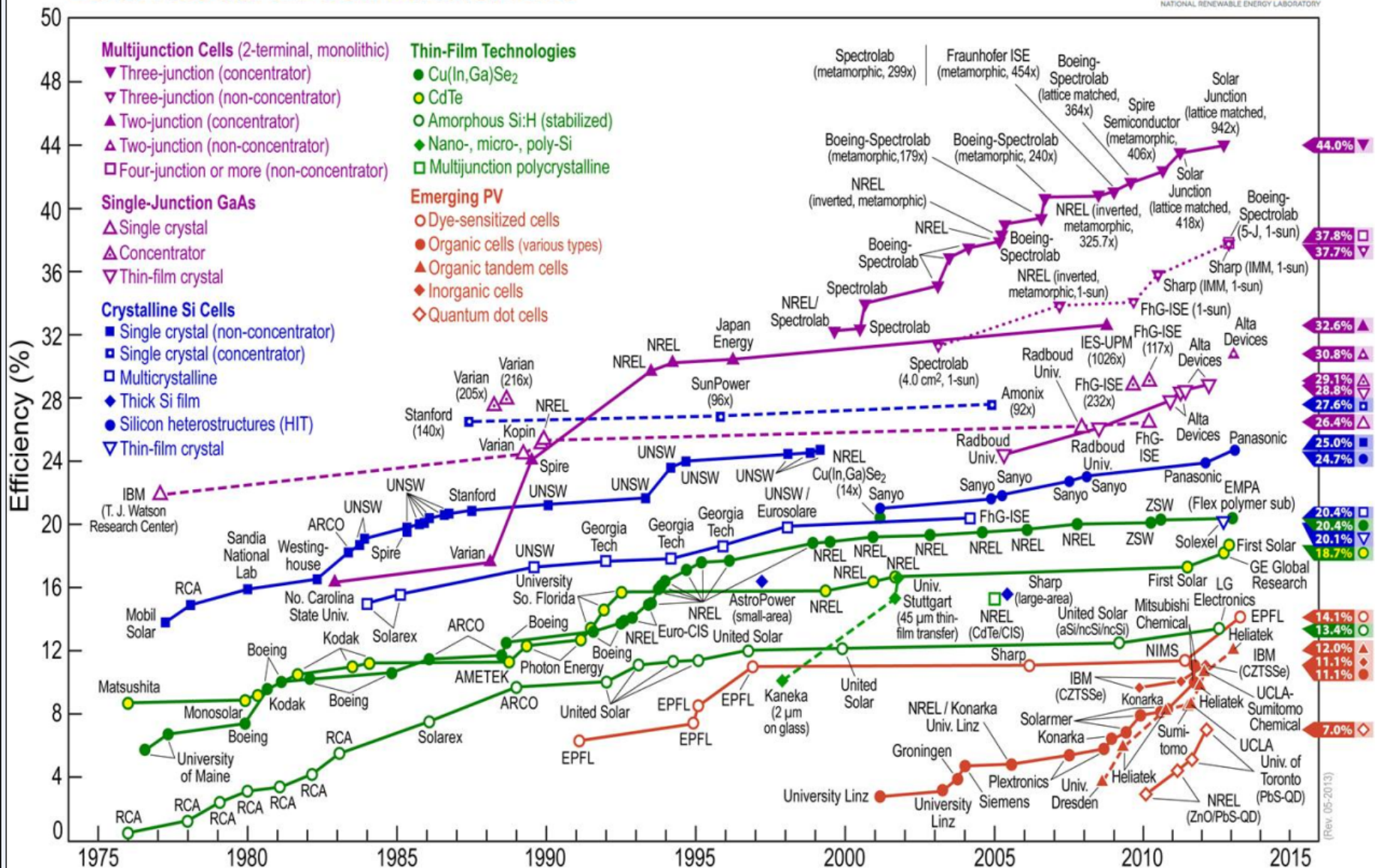


Maximum theoretical solar cell efficiency (under AM 1.5 G) as a function of energy gap of the absorber

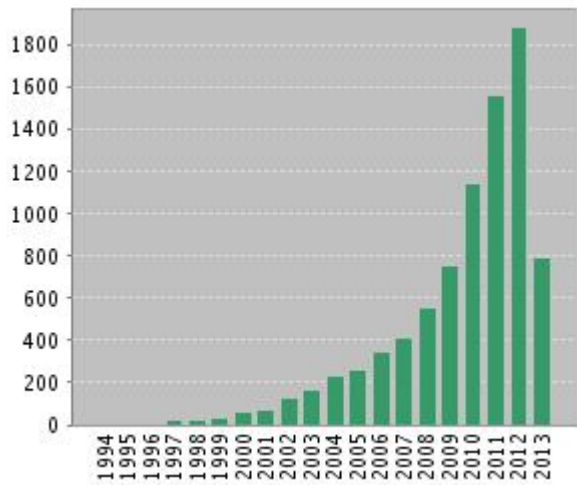
minimizing energy losses in DSCs

dyes with tunable gap
 redox couples
 electrodes
 interfaces

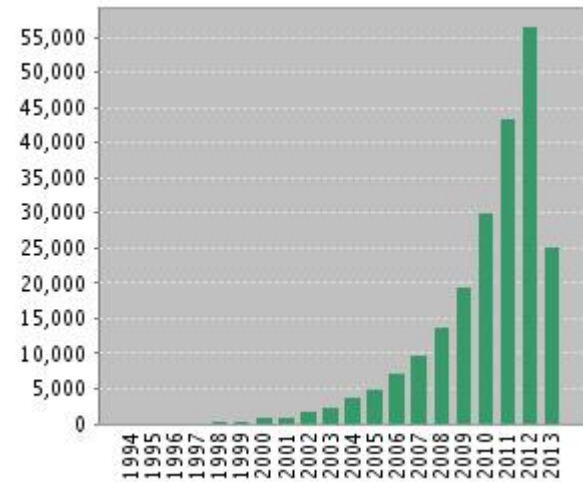
Best Research-Cell Efficiencies



Dye sensitized solar cells (Publications vs. Citations)



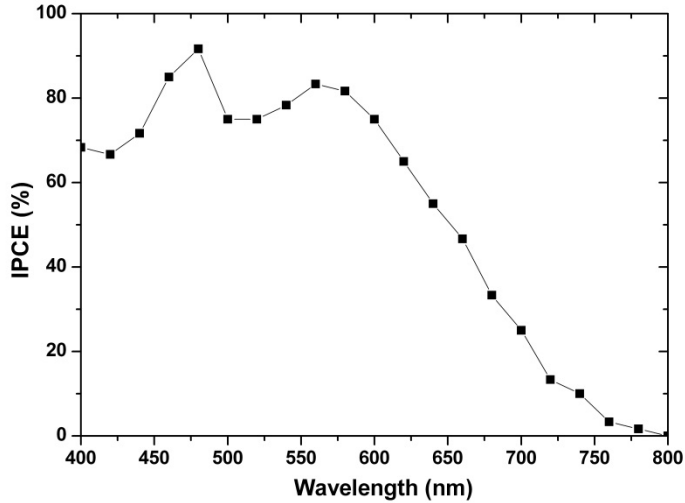
Publications 8489



Citations 221901



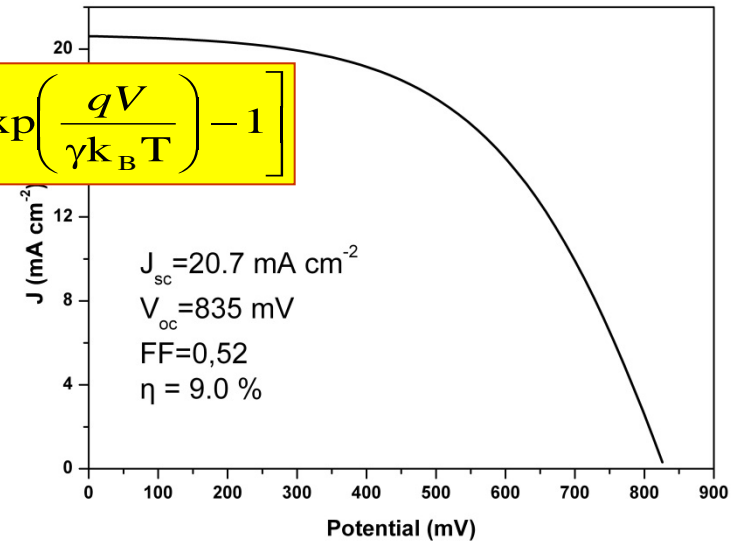
DSC parameters



$$IPCE(\%) = \frac{1240 \cdot j(\mu A / cm^2)}{P(W / m^2) \lambda(nm)}$$

$$IPCE(\lambda) = LHE(\lambda) \times \Phi_{inj} \times P_{coll}$$

$$I(V) = I_{sc} - I_0 \left[\exp\left(\frac{qV}{\gamma k_B T}\right) - 1 \right]$$



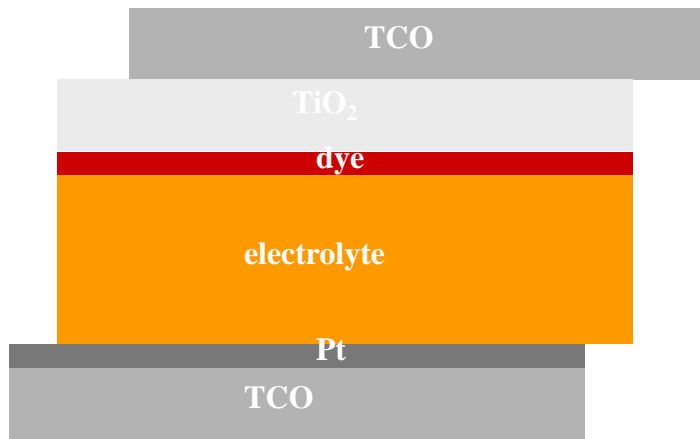
$$J_{sc} (\text{mA} \cdot \text{cm}^{-2})$$

$$V_{oc} = \frac{\gamma k_B T}{q} \ln\left(\frac{I_{sc}}{I_0} + 1\right)$$

$$FF = \frac{P_{max}}{V_{oc} I_{sc}} = \frac{V_m \cdot I_m}{V_{oc} \cdot I_{sc}}$$

$$\eta = \frac{P_{max}}{P_s} = \frac{FF \cdot V_{oc} \cdot J_{sc}}{P_s}$$

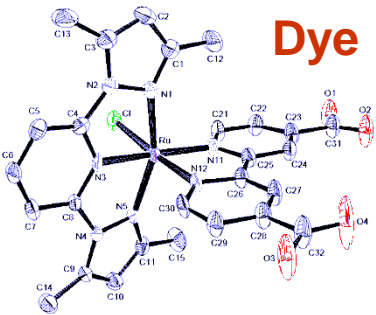
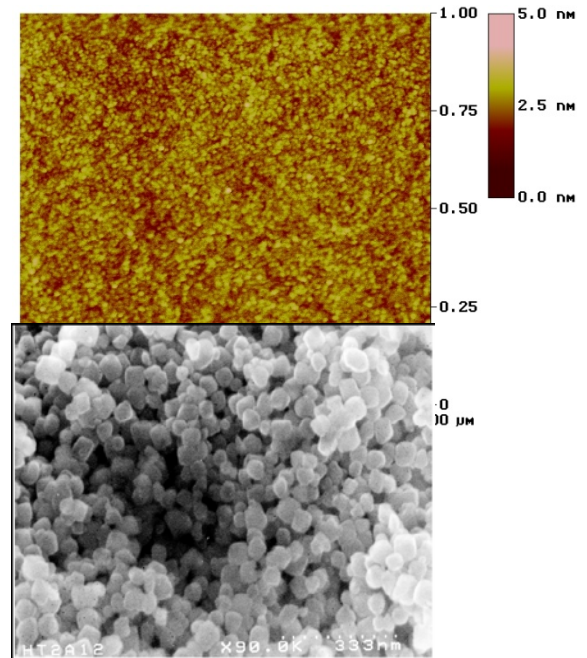
DSC the main elements



Semiconductor

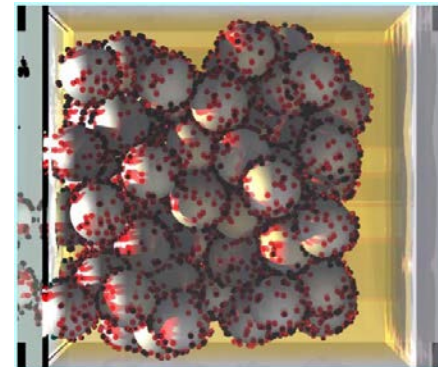
Nanocrystalline
Mesoporous

morphology
particle size



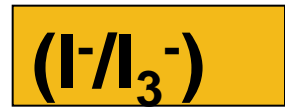
Requirements of the Sensitizer

- panchromatic, i.e. absorb visible light of all colors
- suitable ground- and excited state redox properties
- thermal and photochemical stability
- firmly grafted to the semiconductor oxide surface
- inject electrons with a quantum yield of unity
- molecular structure to minimize recombination



Electrolyte

- redox potential
- conductivity
- reversibility
- stability
- recombination effects, passivation, interface energetics,...



Optimization of the semiconducting electrode TiO₂ Nanoparticles

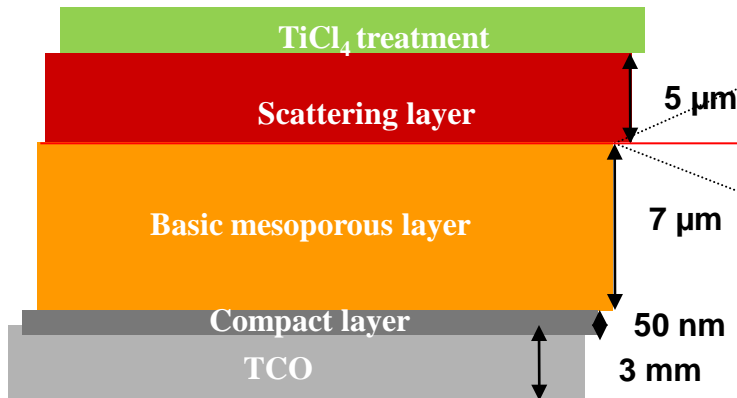
TiO₂ the material of choice

Non toxic

Photochemically stable

Can be tailored in nanoscale

TiO₂ electrode: Complex structure

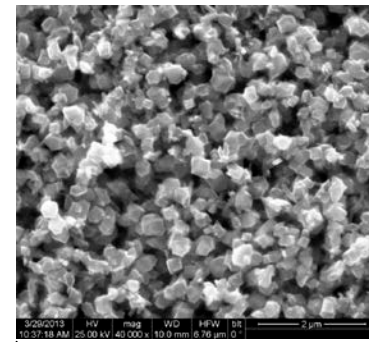


Compact layer: block recombination through exposed back-contact

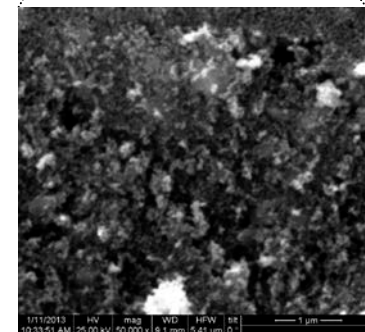
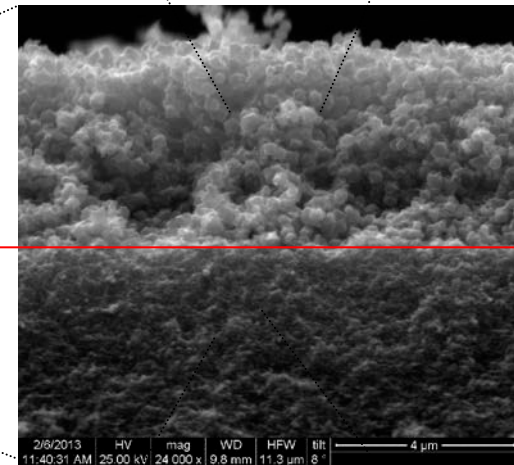
Basic mesoporous layer: active layer with high surface area to adsorb maximum dye

Scattering layer: bigger particles to scatter light and enhance light harvesting

TiCl₄ post-treatment: creates a monolayer of TiO₂ nanoparticles (1-2 nm) around the TiO₂ crystallites, enhancing electron injection, reducing interfacial recombination



Particles
150-250 nm



Nanoparticles
12-13 nm
Porosity 68%

Optimization of the semiconducting electrode Titania nanotubes (TiNTs)

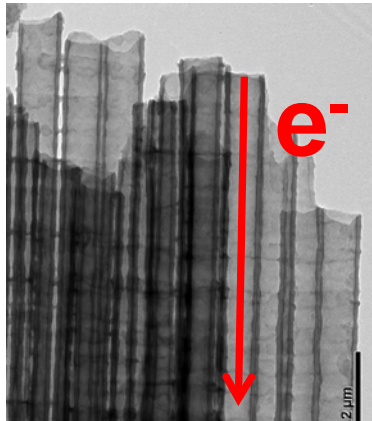
TiNTS: Advantages

- Excellent electric contact with the substrate
- Enlarged porosity, surface area and material density
- High surface roughness (dye loading)
- Direct pathways for species (electrons) diffusion
- Flexible solar cells

Nanotubes
VS
Nanoparticulate
films

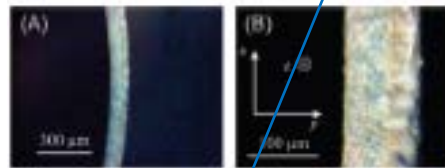
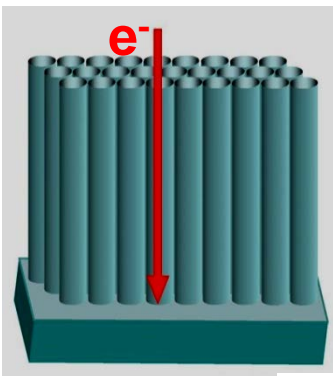
Vertically oriented NT arrays

- Self-organization
- Open morphology, ordered structure
- Low charge recombination losses
- Most favorable nanostructure

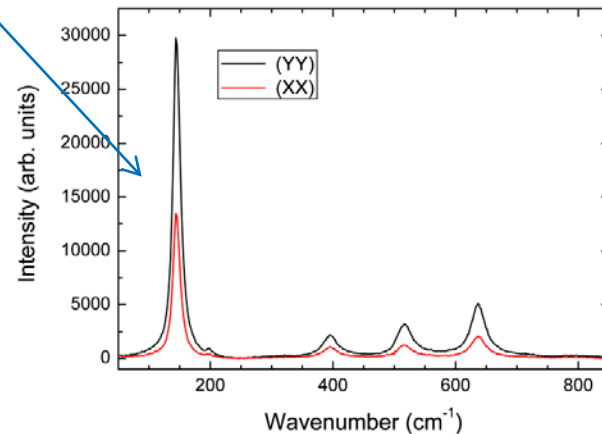


Vectorial charge transport

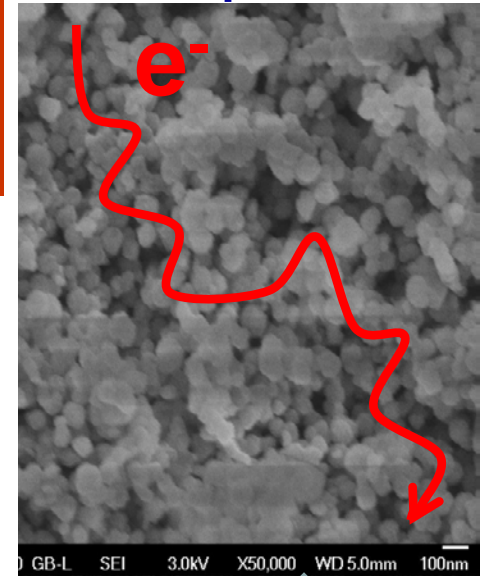
Antenna effect on Ti-nanotubes



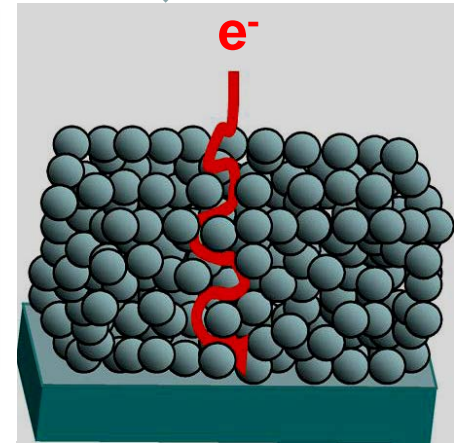
J. Phys. Chem. C 112 (2008) 12687



Sintered Nanoparticles

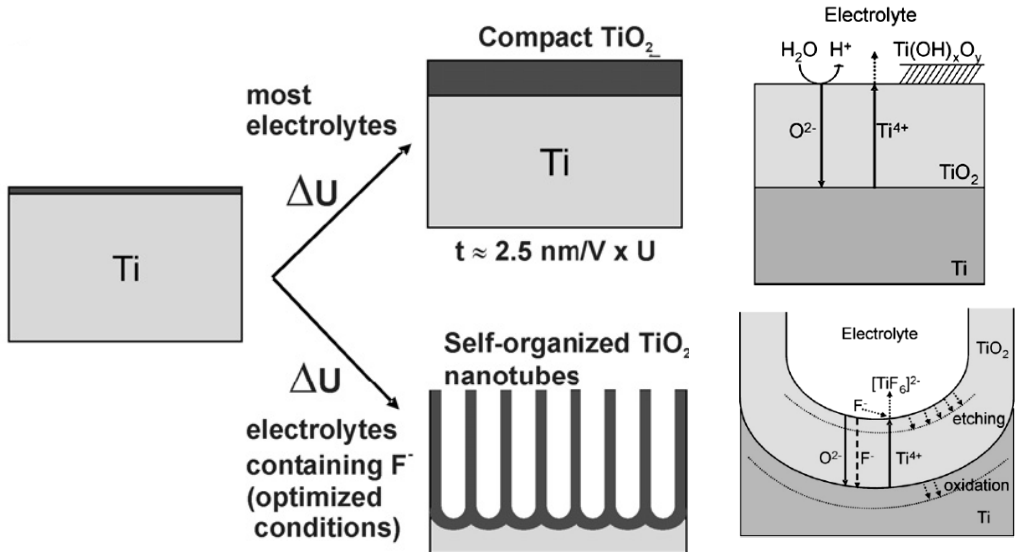
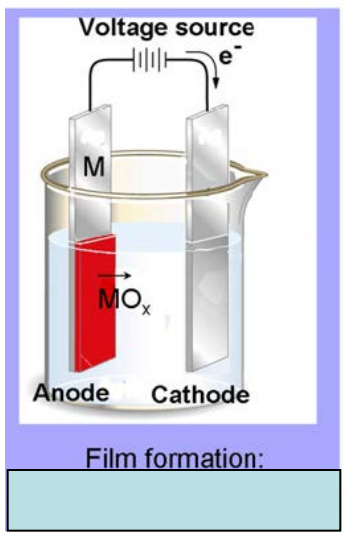


Random walk



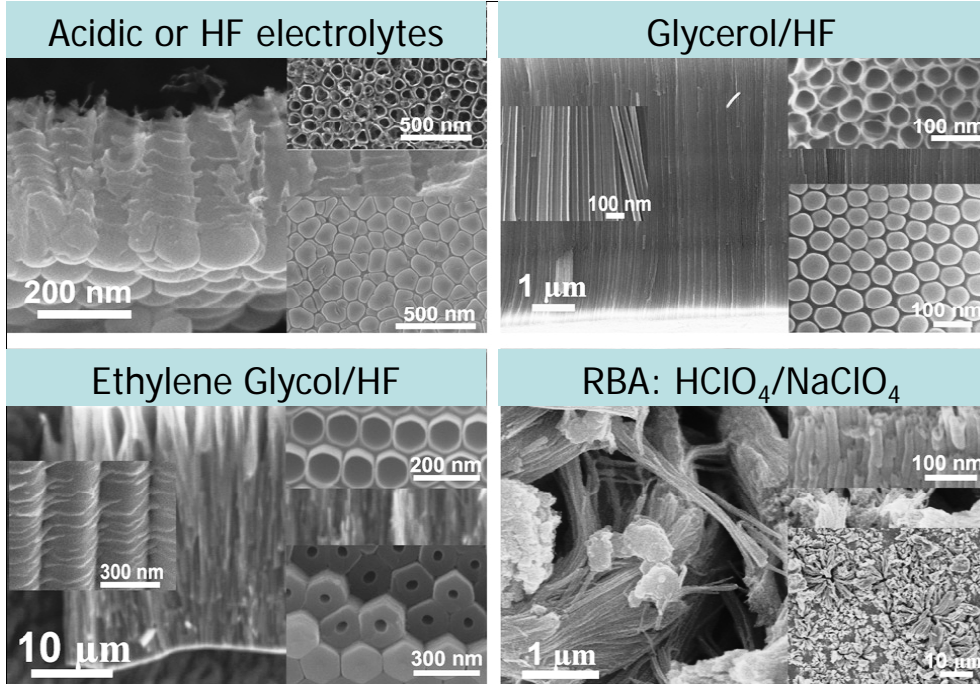
Vertically oriented TiO₂ nanotube arrays grown by electrochemical anodization

Self-organized TiO₂ nanotubes

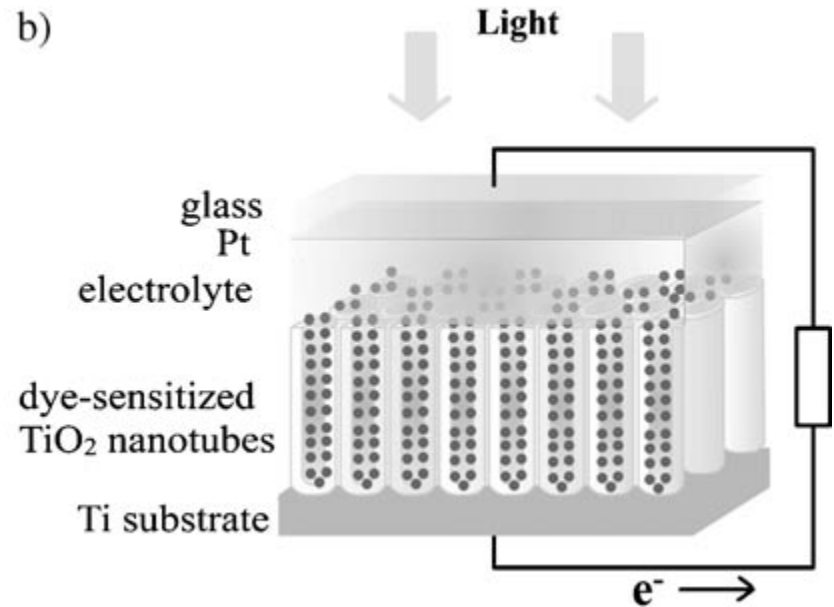
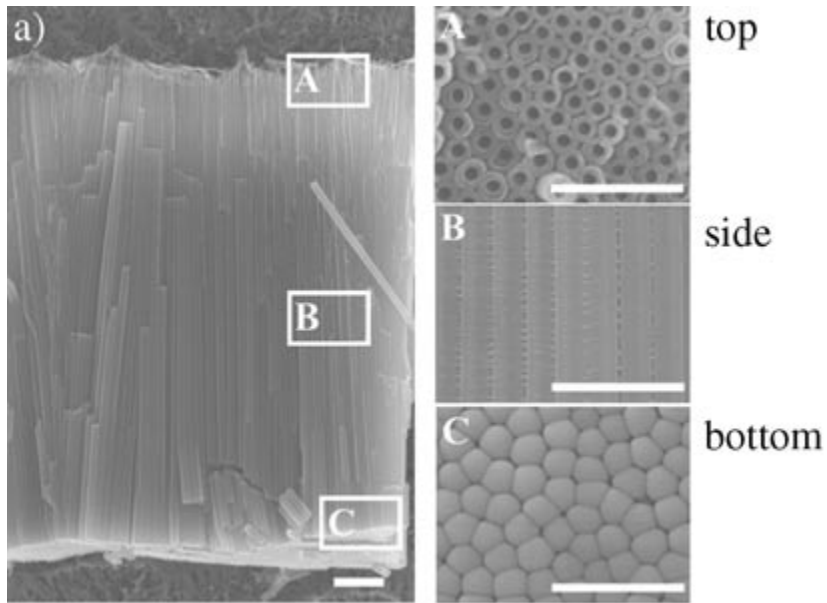


Tailored morphologies

Controlling the anodization conditions of Ti (temperature, applied potential/current, electrolyte species, electrolyte pH, viscosity, aqueous or organic electrolyte etc.), different titanium oxide structures such as a disordered porous layer, a highly self-organized porous layer, or finally a highly self-organized nanotubular array with tailored morphological characteristics can be obtained.



TiO₂Nanotubes in DSC: Critical Factors for the Conversion Efficiency

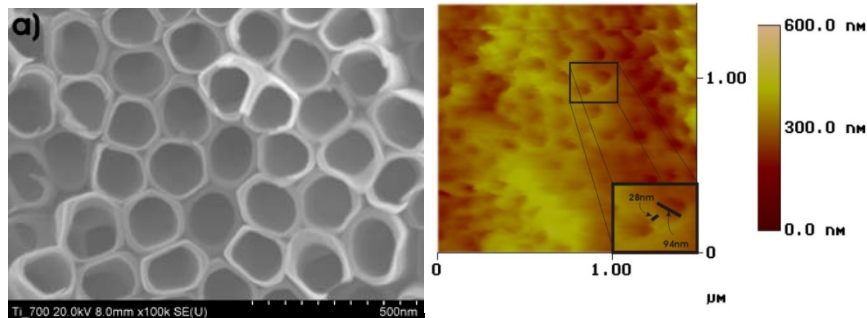
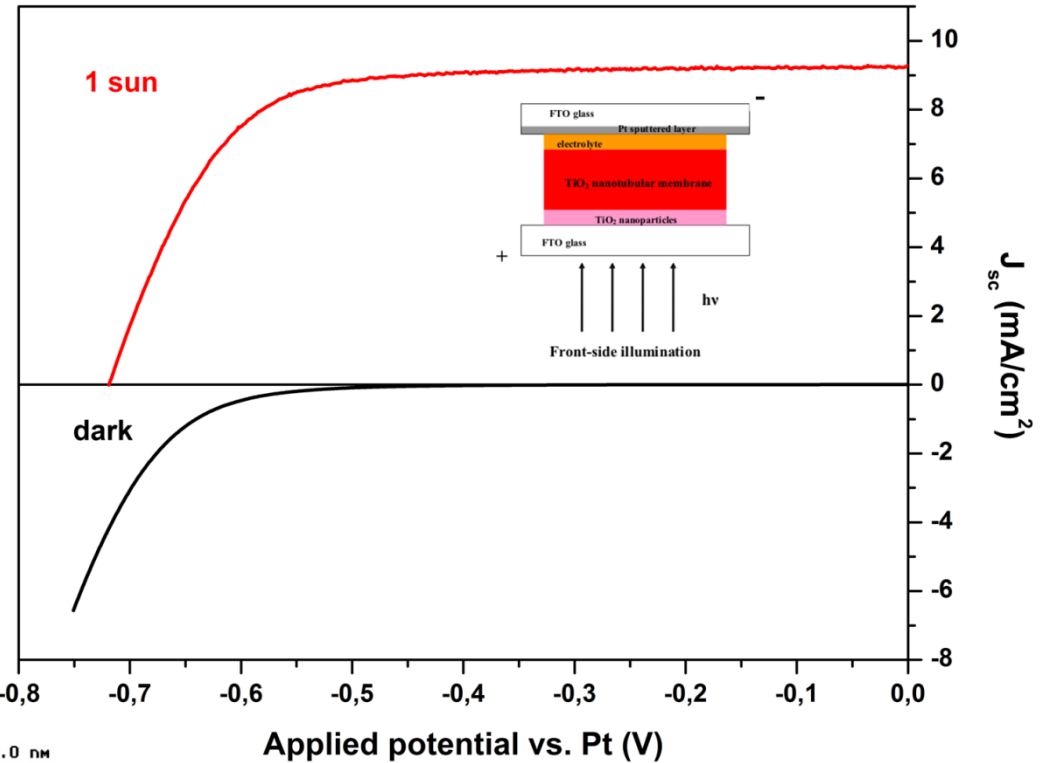
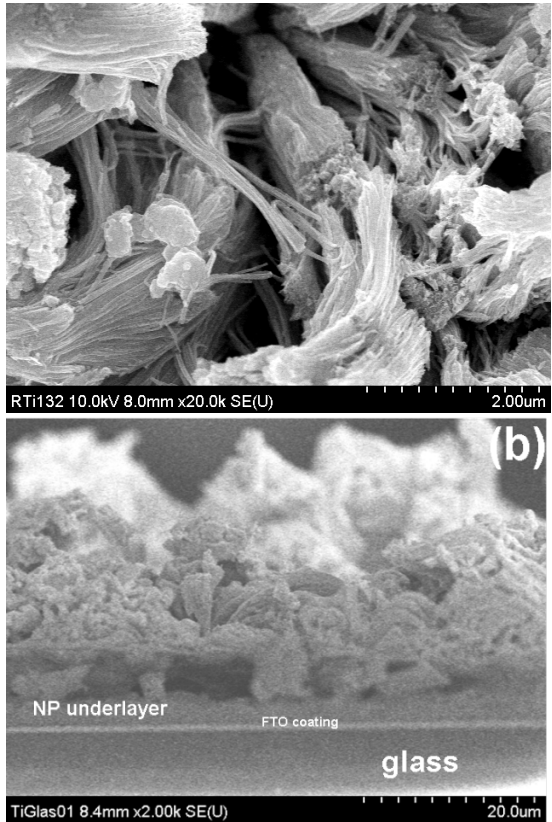


Critical Factors

- morphology
- crystalline structure
- tube length and diameter
- annealing temperature
- TiCl₄ treatment
- dye loading

Bundle shaped titania NT membranes on FTO glass

Chemical lifting off the tubes and deposition of the free-standing membrane onto the conductive substrate, using a nanoparticulate paste as a “glue”

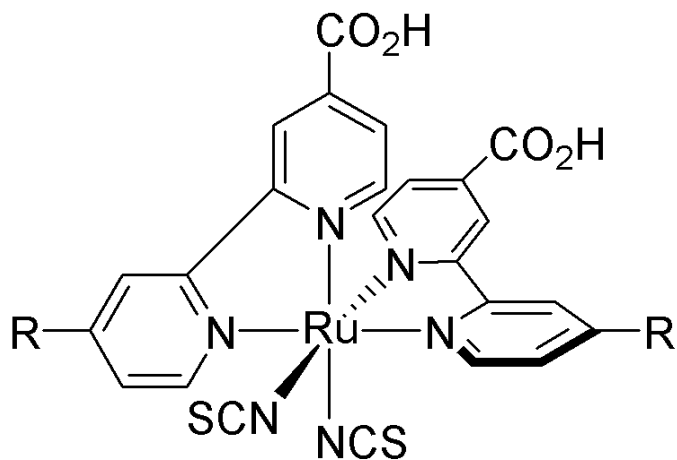
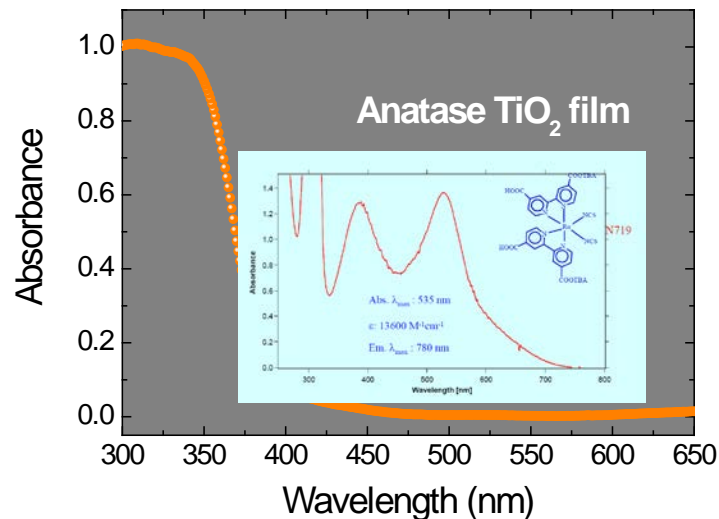
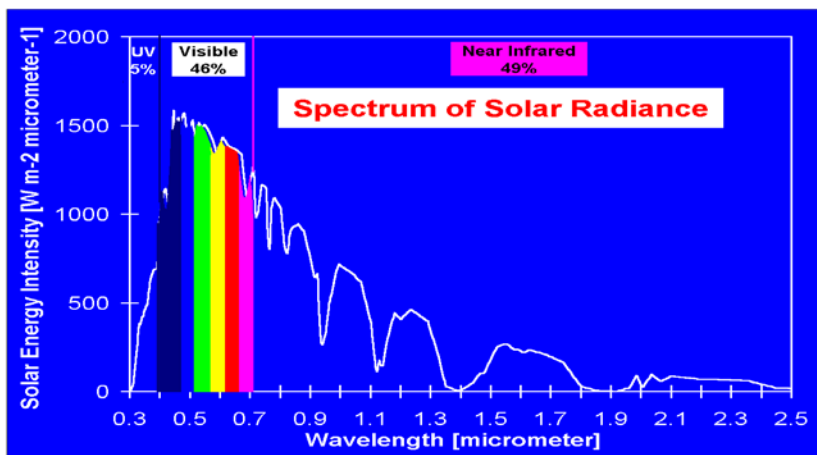


- Front side illumination
- High efficiencies up to 4.7 %

Conclusions (titania nanotubes)

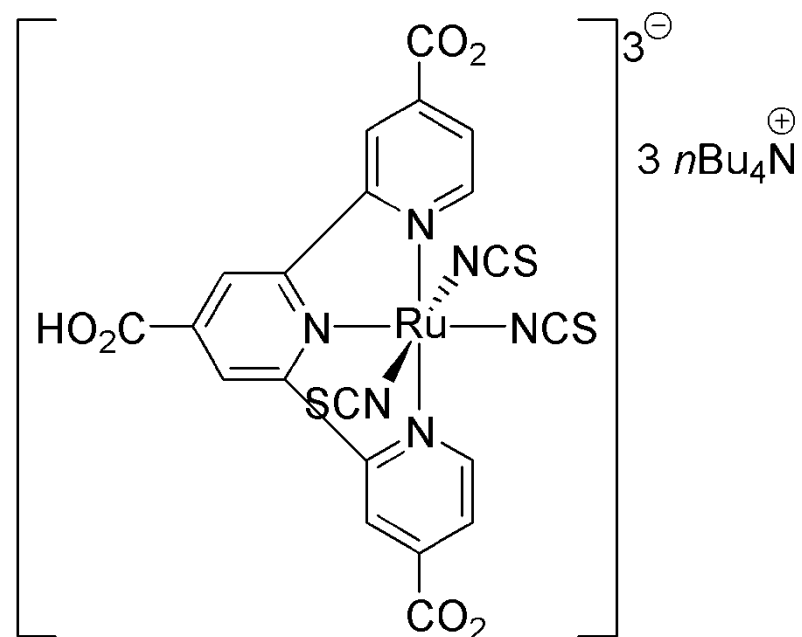
- 1-D self organized TiO_2 nanostructures are formed by electrochemical anodization of Ti in electrolytes containing F- anions
- The NTs morphology, length and wall thickness can be efficiently controlled by appropriate choice of potential/current density, anodization time, solvent nature, water content, F- concentration
- The anodized materials are amorphous and transform to the anatase phase following thermal treatment at 450 °C
- Besides the tubes inherent flexibility and vectorial electron transport, nanotubular NT membranes can be efficiently transferred on conductive glass substrates
- The TiO_2 NTs can be efficiently sensitized by molecular dyes and the corresponding DSCs present high power conversion efficiencies

Dye sensitization: Overcoming critical 10 % with Ru(II)-dyes



N3 : R = CO₂H

N719 : R = CO₂⁻ N⁺(n-Bu)₄ **11.2 %**

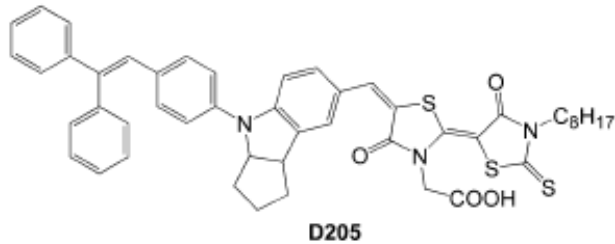


1 (black dye) **10.4%**

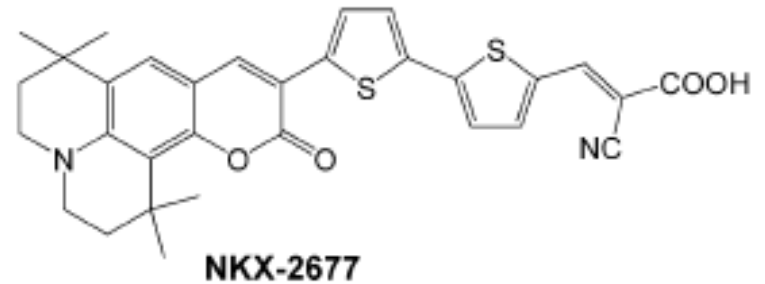
Organic dyes to promote light harvesting

High extinction coefficients (ϵ)

indoline



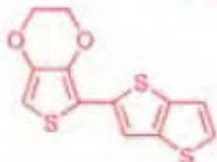
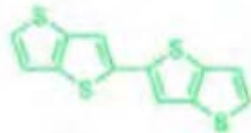
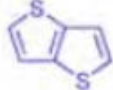
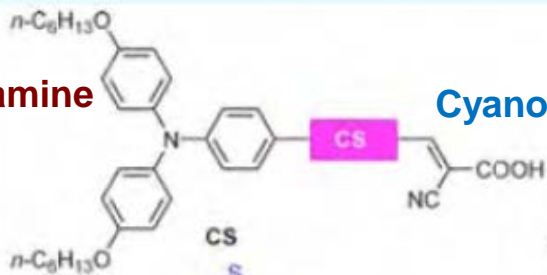
coumarin



Donor- π -bridge-acceptor (D- π -A)

triphenylamine

Cyanocrylic acid

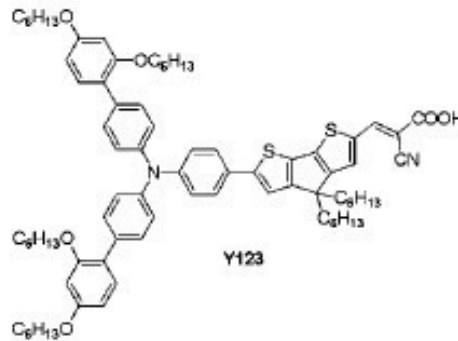


Dye

C206

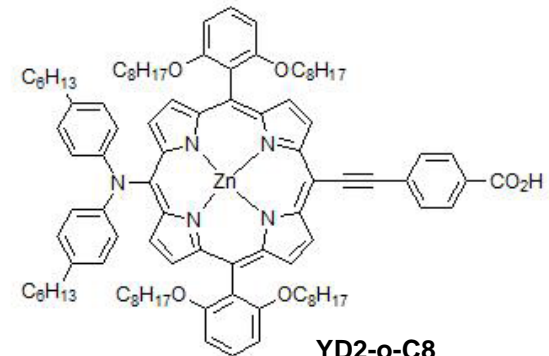
C211

C217



Y123

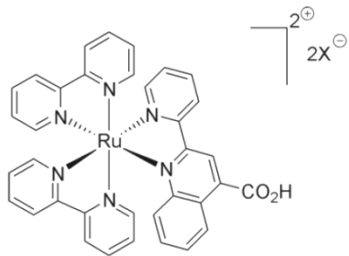
Zn-porphyrins



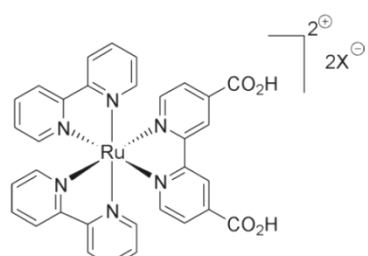
YD2-o-C8

Thiophenes as linkers

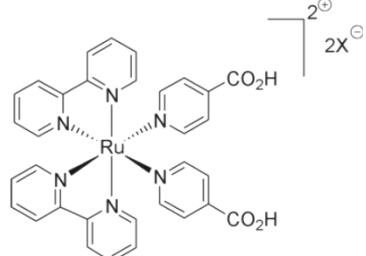
TAILOR-DESIGNED DYES FOR DSCs (NCSR Demokritos)



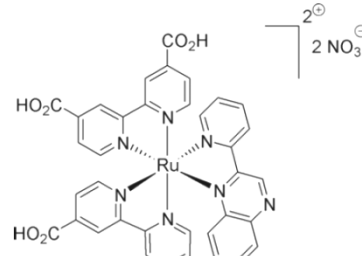
4 : X = Cl
5 : X = PF₆



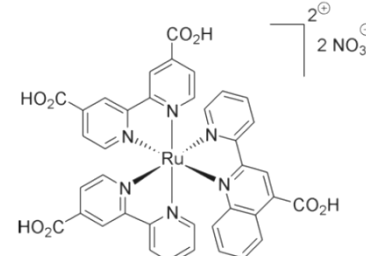
6 : X = Cl
7 : X = PF₆



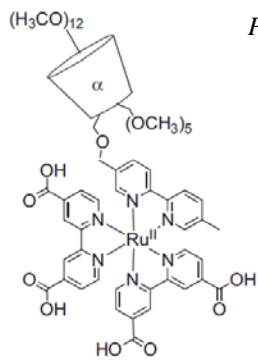
8 : X = Cl
9 : X = PF₆



10

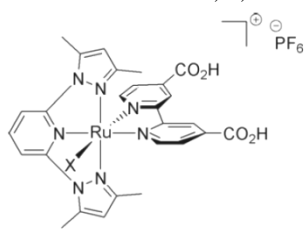


11

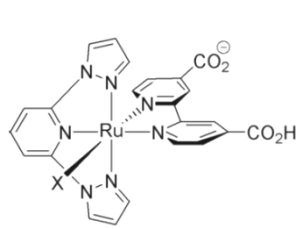


1-α-CD

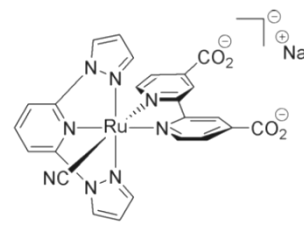
Photochem. Photobiol. Sci. **2009**, 8, 726



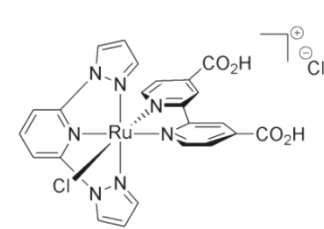
12 : X = Cl
13 : X = NCS



14 : X = Cl
15 : X = NCS



16



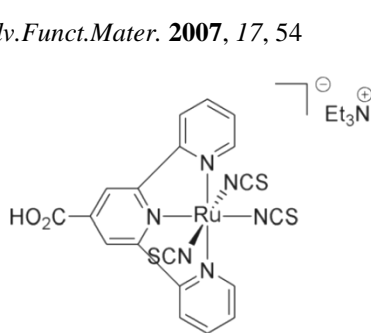
17

Inorg. Chim. Acta **2002**, 328, 204

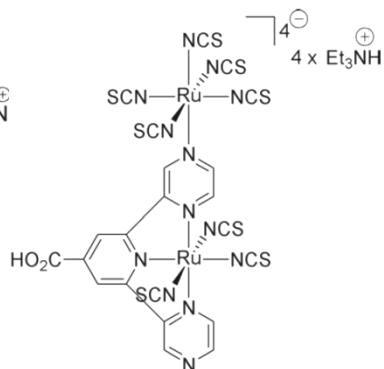
Polyhedron **2002**, 21, 2773

Eur. J. Inorg. Chem. **2007** 5633

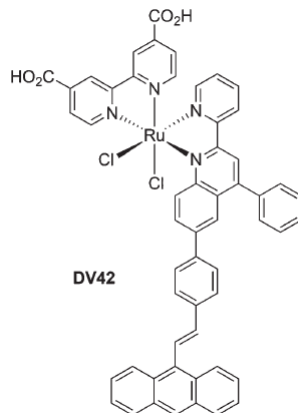
Adv. Funct. Mater. **2007**, 17, 54



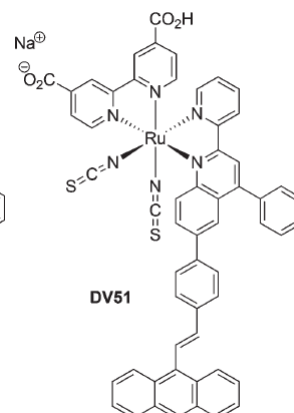
18



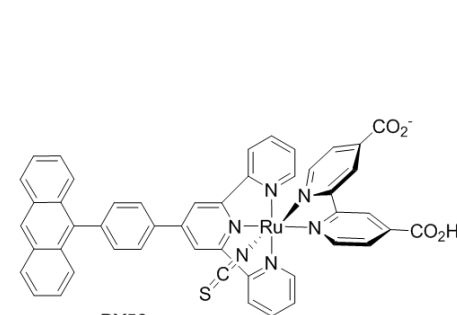
19



DV42



DV51



DV56

Manuscript in preparation

J. Photochem. Photobiol. A: Chem. **2010**, 214, 22

Coordination Chemistry Reviews **255 (2011) 2602– 2621**

Dalton Trans. **2013**, 42, 6582

INNOVATIVE ELECTROLYTES FOR DSCs (NCSR Demokritos)

Code name for electrolyte	Composition	Efficiency (mean value)
BlendB	<ul style="list-style-type: none"> PMII/EMIDCA (13:7 v/v) I₂ (0.2 M) LiI (0.1 M) 4TBP (0.4 M) 	3.5%
BlendE-noLiI	<ul style="list-style-type: none"> DMII/EMIDCA (13:7 v/v) I₂ (0.2 M) GuSCN (0.2 M) 4TBP (0.4 M) 	3.5%
D1	<ul style="list-style-type: none"> DMII (1 M) I₂ (0.015 M) LiI (0.05 M) GuSCN (0.1 M) 4TBP (0.5 M) in MPN (85:15)	5.5%
Z946	<ul style="list-style-type: none"> DMII (1 M) I₂ (0.15 M) GuSCN (0.1 M) NMBI (0.5 M) in MPN	4.5%
DD1	<ul style="list-style-type: none"> DMII (1 M) I₂ (0.03 M) LiI (0.05 M) GuSCN (0.1 M) 4TBP (0.5 M) in MPN (85:15)	6%
Super liquid	<ul style="list-style-type: none"> DMII (1 M) I₂ (0.015 M) LiI (0.05 M) GuSCN (0.1 M) 4TBP (0.5 M) in ACN/valeronitrile (85:15)	6%
ENF	<ul style="list-style-type: none"> PMII (0.8 M) I₂ (0.02 M) CsI (0.1 M) 4TBP (0.45 M) in PC + 4.5% w/w PEO 2.000.000	3.5%
ENF-NMBI	<ul style="list-style-type: none"> PMII (0.8 M) I₂ (0.02 M) CsI (0.1 M) NMBI (0.45 M) in PC + 4.5% w/w PEO 2.000.000	4.2% (sealed) 4.6% (open)
A2	<ul style="list-style-type: none"> PMII/EMII in TCB (13:7 w/v) I₂ (0.2 M) LiI (0.1 M) 4TBP (0.4 M) + 6% w/w silica S-5130	4%

redox couple, solvent, additives

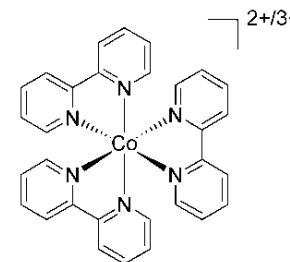
Iodine-based

- Solvent-based liquid (MPN, ACN/Valeronitrile)
- Solvent-free (ionic liquid based): DMII, MPII, MPII/EMIDCA, DMII/EMIDCA
- Additives: 4-TBP, GuSCN, NMBI (physisorption, negative shift of TiO₂ CB)

Iodine-free

Coordination compounds with redox potential > E (iodide/triiodide)

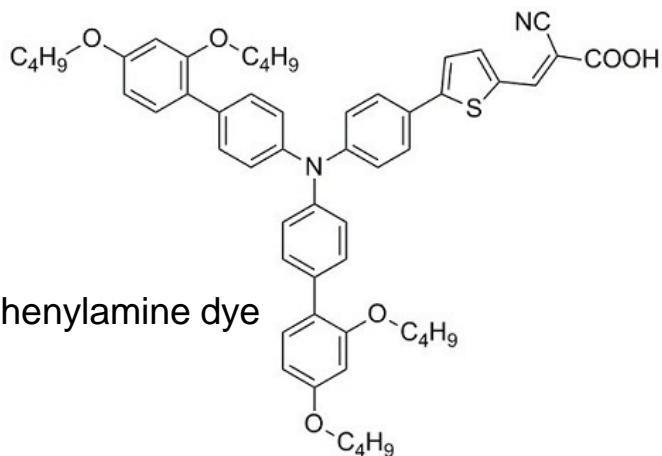
- Cobalt-based (Co²⁺/Co³⁺) + organic dyes (Voc~1.0 V)



Solidified

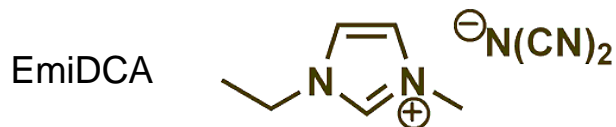
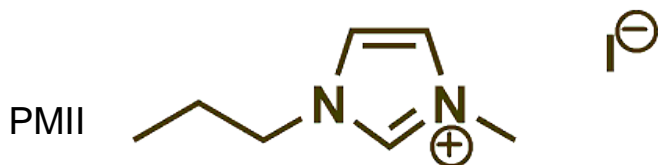
- PEO (+ fillers)
- Silica

Combining TiO₂ surface-blocking organic sensitizer and solvent-free ionic liquid-based redox electrolytes

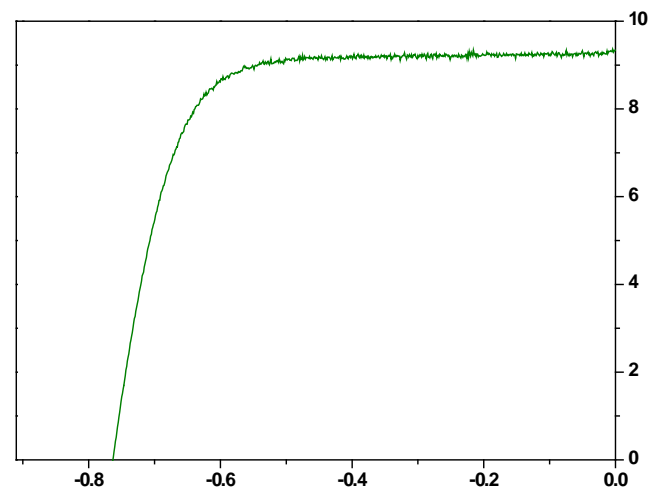


D35 triphenylamine dye

Dye-Electrolyte	J _{sc} (mA/cm ²)	V _{oc} (V)	FF	η (%)
D35-IL	9.3	0.76	0.73	5.2
D35-liquid B	10.7	0.74	0.73	5.8
D35 liquid A	11.1	0.79	0.73	6.4
Z907-IL	11.4	0.71	0.71	5.8
Z907-liquid A	15.5	0.76	0.71	8.3

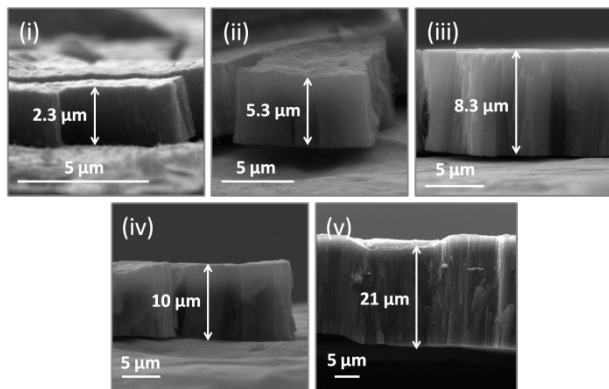


13:7 blend of PMII with EmiDCA as IL electrolyte (and additives)

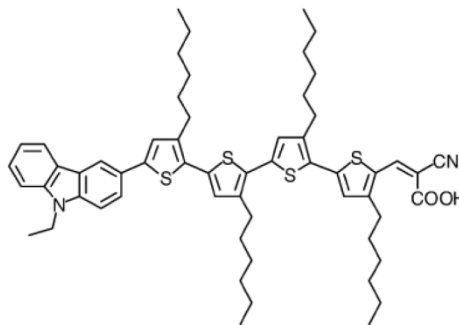


OPTIMIZATION OF ANODIC TITANIA NANOTUBES FOR DYE SOLAR CELLS USING COBALT(II)/(III) ELECTROLYTES

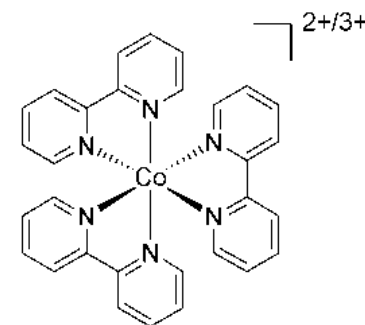
TiO₂ nanotubes



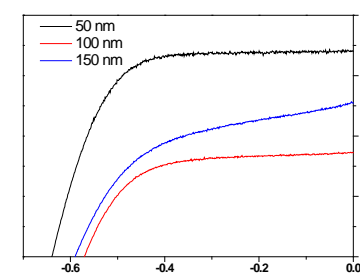
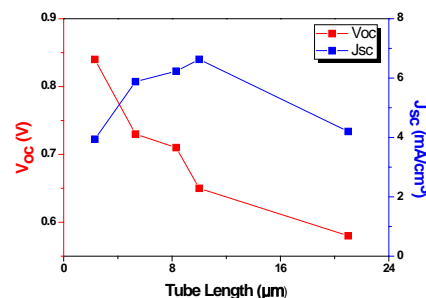
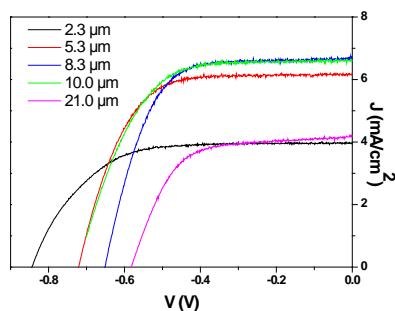
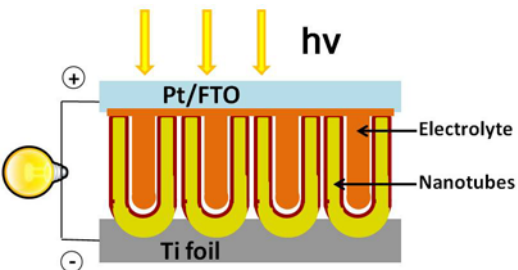
MK-2 Organic Dye
 $\epsilon = 38.400 \text{ M}^{-1} \text{ cm}^{-1}$ @ $\lambda_{\text{max}} = 480 \text{ nm}$



Cobalt^{2+/3+} Redox Couple
 in acetonitrile (with LiClO₄ and TBP)



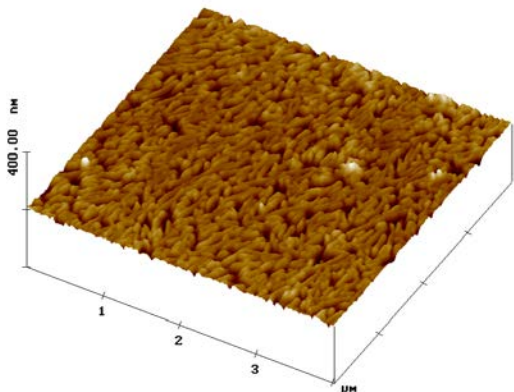
Back-Illuminated Solar Cell



Solar Cell Parameters	Tube Length (μm) (D~50 nm)					Tube Diameter (nm) (L~10 μm)		
	2.3	5.3	7.3	10.0	21.0	50	100	150
J_{sc} (mA/cm²)	3.94	5.88	6.23	6.63	4.20	6.81	3.45	5.09
V_{oc} (V)	0.84	0.74	0.71	0.65	0.58	0.64	0.57	0.59
FF	0.65	0.66	0.64	0.67	0.63	0.68	0.63	0.50
η (%)	2.17	2.86	2.81	2.88	1.54	2.95	1.24	1.52

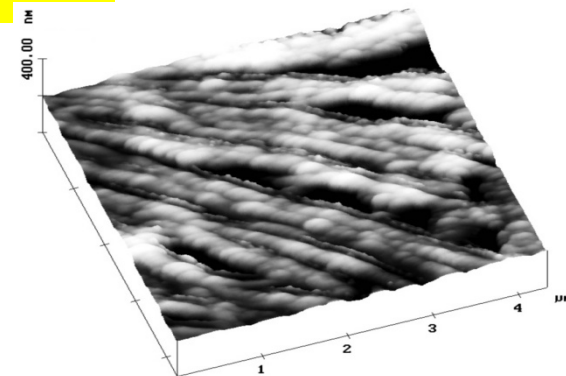
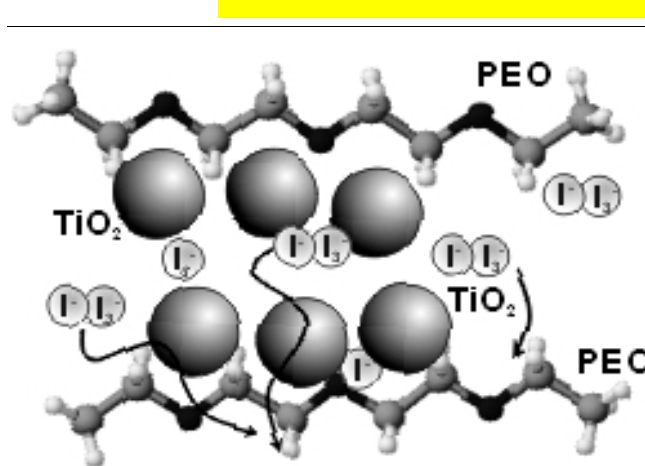
Solidification: Development of solvent-free composite polymer (PEO) redox (I^-/I_3^-) electrolytes

initial PEO

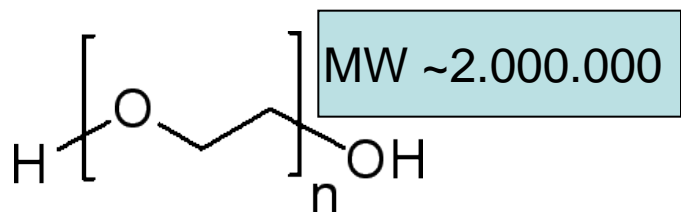


high degree of crystallinity

Redox electrolyte

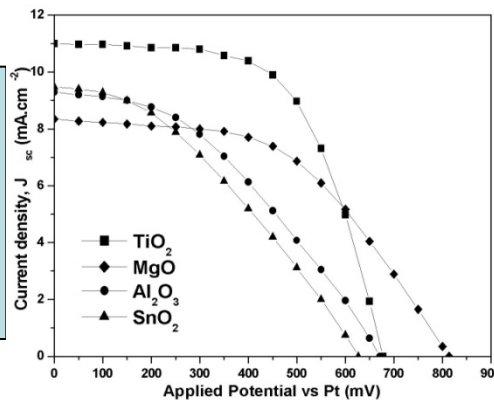


$DI_3^- : 2 \times 10^{-6} \text{ cm}^2 \text{ s}^{-1}$
 $\sigma : 1.5 \text{ mS cm}^{-1}$
 high amorphicity

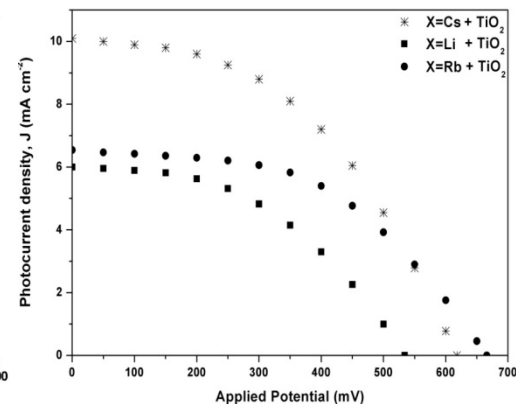


- Addition of solid plasticizers (fillers)
- Filler: Metal oxide nanoparticles
- Dispersion of the I^-/I_3^- redox couple

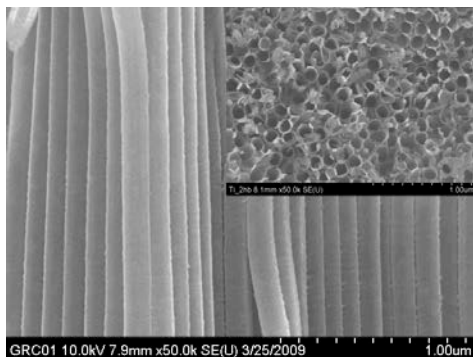
filler effect



cation effect

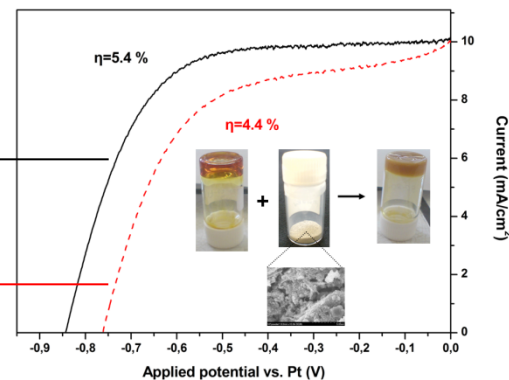


Solidified polymer redox electrolytes, filled with NTs



with filler

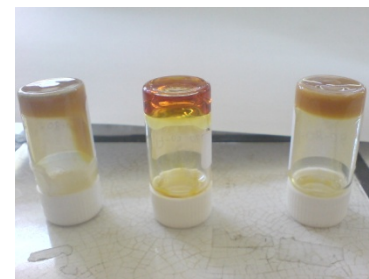
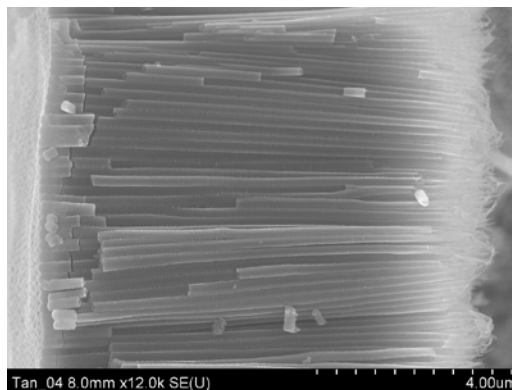
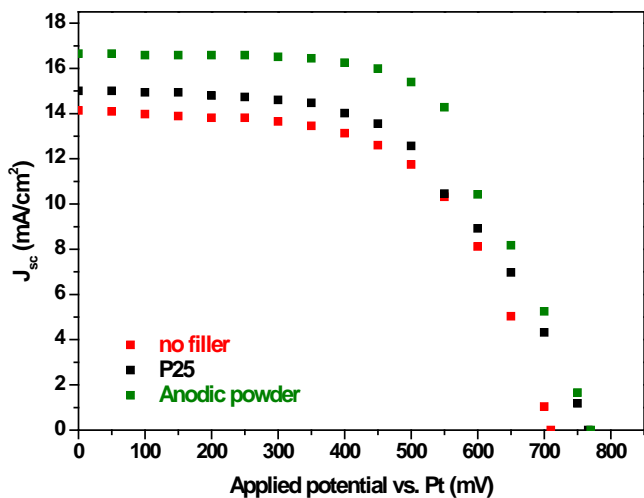
No filler



Advanced Energy Materials, 1 (2011) 569-572

Electrolyte: MPlI, CsI, I₂, 4TBP, PEO

optimization



η = 7.8 %, the highest efficiency ever reported for a solidified polymer electrolyte

Preparation of SiO₂ electrolytes

1st step

preparation of elementary electrolyte → dissolution of I₂ in solvent, through stirring at room temperature



Fig.1 Reference Liquid electrolyte

2nd step

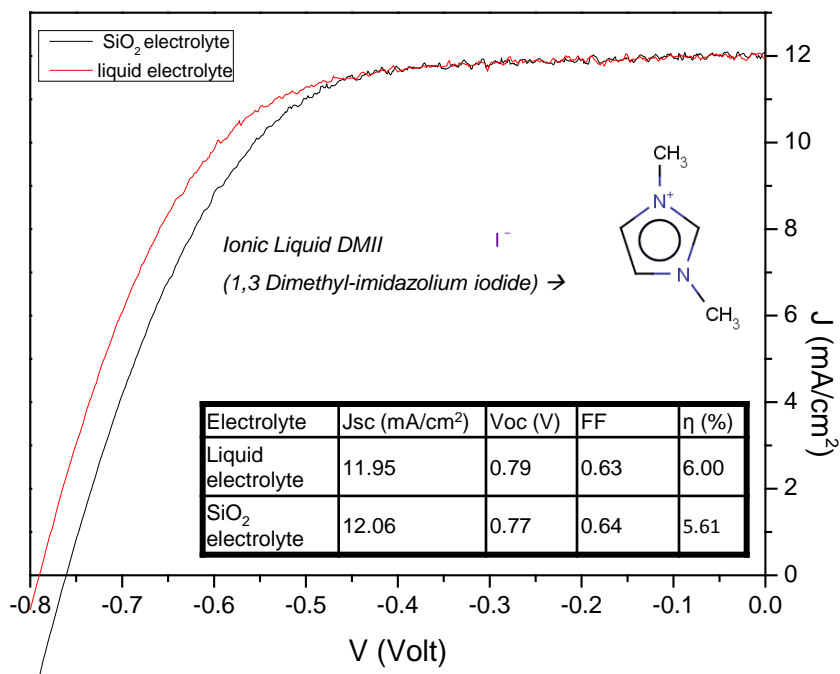
additive addition → dissolution of additives, through stirring and with slight heating (~50° C)



Fig.2 Solidified electrolyte with 6% w/v iSiO₂ nanoparticles

3rd step

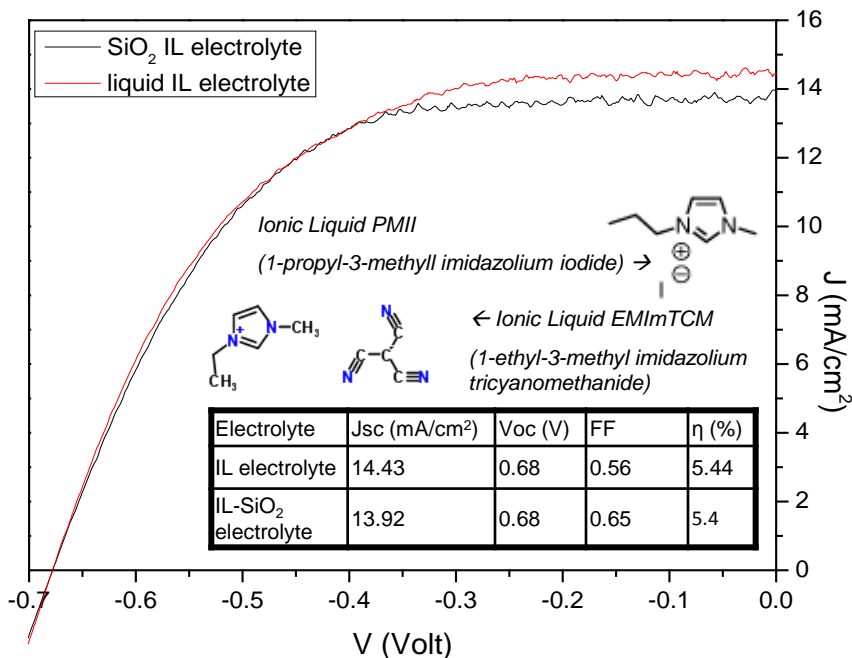
solidification → after obtaining a homogenous liquid (step 2) the electrolyte is left at room temperature to cool down. Then SiO₂ is added to the mixture gradually, under stirring, until solidification is complete



Composition of MPN based electrolyte (left) :

DMII (1 M) / I₂ (0.015 M) / LiI (0.05 M) / GuSCN (0.1 M) / 4TBP (0.5 M) in MPN

Solidification was achieved with addition of 7% w/v silica S-5130



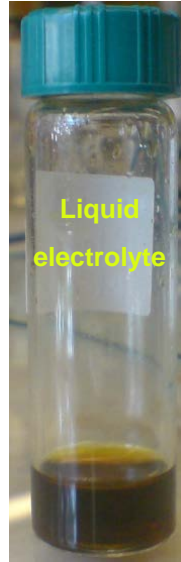
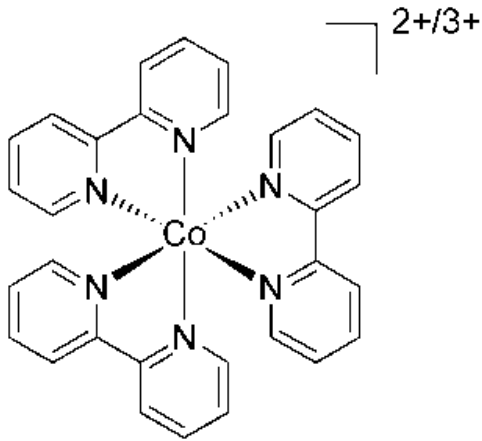
Composition of solvent free electrolyte (right) :

PMII : EMImTCM (13:7 v/v) / I₂ (0.2 M) / LiI (0.1 M) / 4TBP (0.4 M)

Solidification was achieved with addition of 5% w/v silica S-5130

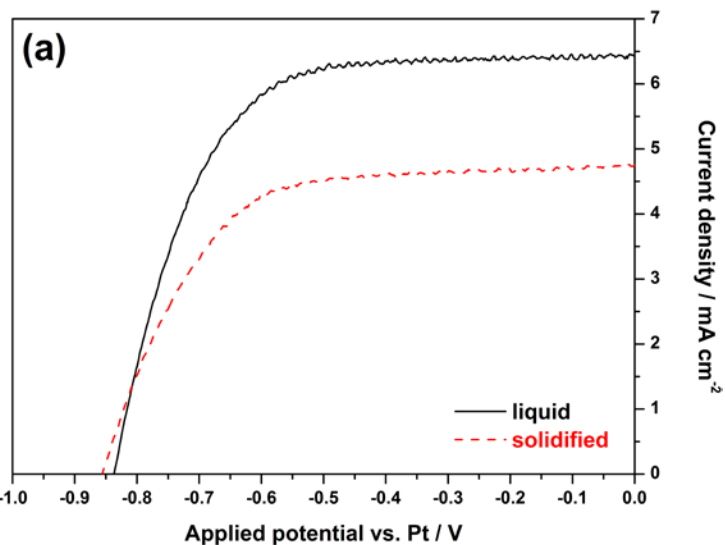
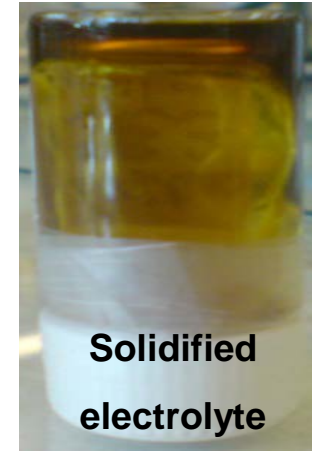
Solidified Co(II)/Co(III)-based electrolytes

0.22 M [Co-(bpy)₃(PF₆)₂]
 33 mM [Co(bpy)₃(PF₆)₃]
 0.1 M LiClO₄
 0.2 M 4-tert-butylpyridine
 Solvent: MPN



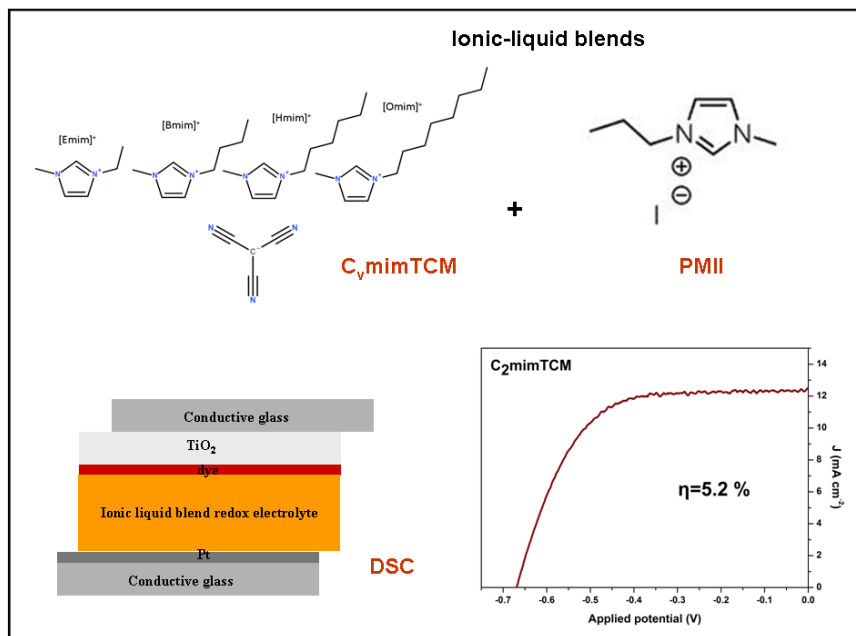
solidified with silica NPs (5% w/w)

+ SiO₂ NPs =



Electrolyte	J _{sc} / mA cm ⁻²	V _{oc} / mV	FF	η / %
Liquid	6.42	836	0.66	3.52
Solidified	4.76	855	0.63	2.58

Binary mixtures of 1-alkyl-methylimidazolium tricyanomethanide $C_v\text{mimTCM}$ with 1-methyl-3-propylimidazolium iodide MPII



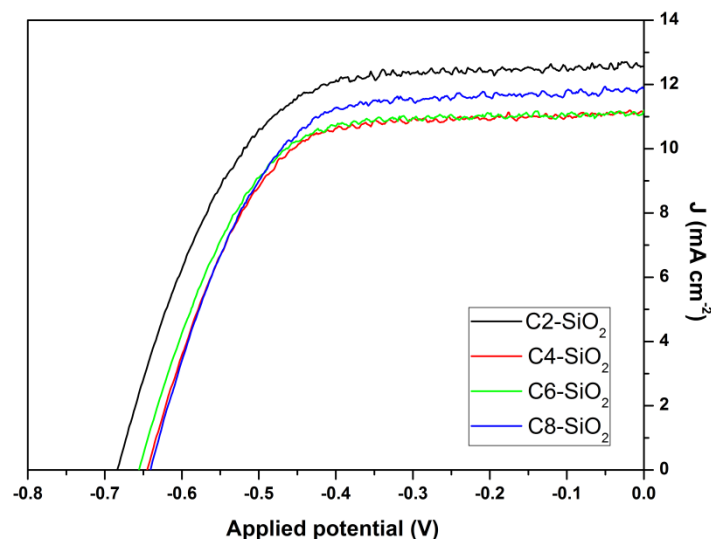
$\text{MPII} / C_v\text{mimTCM} = 13:7$

0.1 M LiI

0.2 M I_2

0.4 M 4-TBP

Modify the alkyl chain length
of the $C_v\text{mimTCM}$ component



SiO_2 (5%)



ionic liquid blend electrolytes
solidified with silica

Conclusions (Electrolytes)

Ionic liquids are excellent candidates for solvent-free low-viscosity electrolytes

$\text{Co}^{2+}/\text{Co}^{3+}$ redox couple gives high V_{oc} (open circuit potential values) in combination with organic dyes

Filler, cation and solvent effects on poly(ethyleneoxide)-based nanocomposite electrolytes for dye-sensitized solar cells

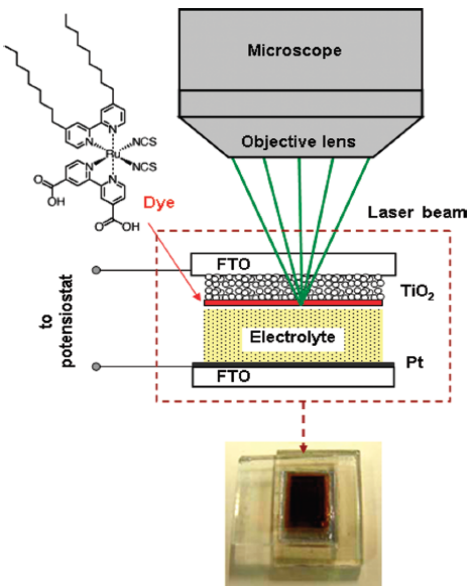
The TiO_2 NTs can be used as fillers in solidified redox active electrolytes and their application results in solid state DSCs with power conversion efficiencies of the order of 8%

Silica solidification very promising results combining the mechanical stability of solids with liquid-like conductivities

Further increase is expected by using TiO_2 NTs in solidified redox electrolytes based on low viscosity ionic liquids

Light and Thermal Stress Effects on Industrial Dye-Sensitized Solar Cells: A Micro-Raman Investigation on the Long-Term Stability of Aged Cells

In-situ Raman Spectrophotoelectrochemistry



Long-term light soaking and thermal stress

Continuous illumination at temperatures of 55-60 °C over 6450 hrs, ~1 sun -Dyesol

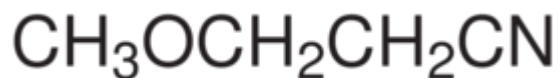
Additional voltage polarization (+0.4 to -0.8 V) -NCSR

- **~10% efficiency decrease (mainly due to J_{sc})**
- **Stability (TiO_2 crystallinity, particle size, dye molecular structure, electrolyte, interfaces)**
- **Reversibility**

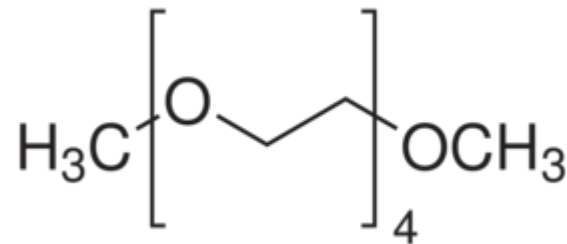
Z907 hydrophobic dye
(I⁻/I₃⁻ MP11, MPN) electrolyte

Solvent effects on stability : MPN vs.TGL

MPN



TGL



Electrolyte	Viscosity mPa s (20 °C)	Boiling point °C	Dielectric constant	Donor number
MPN	1.2	165	36.0	15.4
TGL	4.0	275	Much lower	24

Glymes family (Masayoshi Watanabe group in Yokohama)

J. Phys. Chem. B 2012, 116, 11323–11331

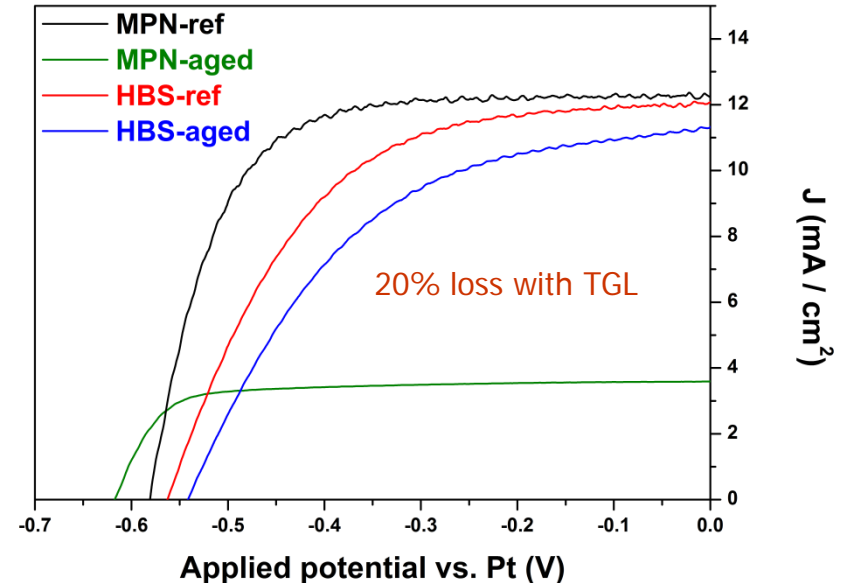
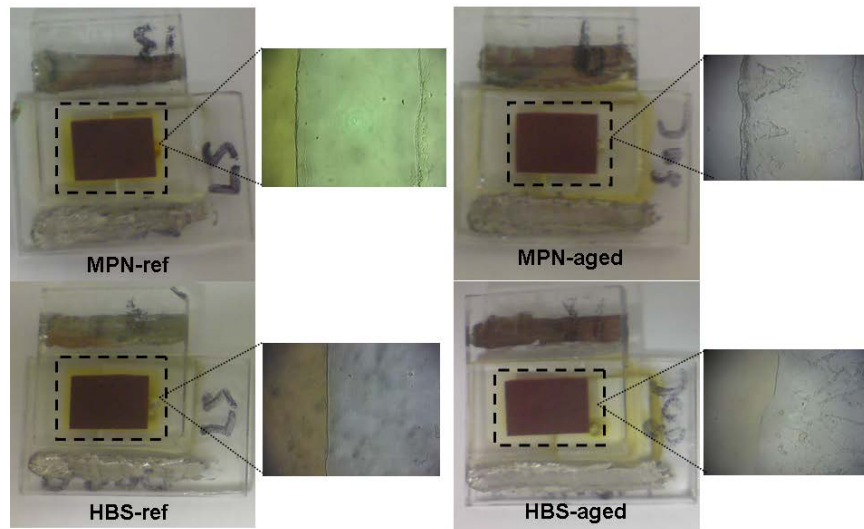
High boiling point solvent

Stability of Dyesol cells using cost-effective components

Prototype cells with **hydrophilic N719** dye (large scale production)

Electrolyte solvents: **low-cost, conventional organic solvents such as MPN or TGL (non-nitrile, HBS solvent)**

Ageing: **light soaking (0.8 sun) for 2000h at MPP**, then **thermal ageing 80 °C dark (2000 h) @ ocp**



The experiment

Batch of 3 identical cells:

Liquid Electrolyte: MP11 + I₂

Solvents: MPN or TGL **comparison**

Additives: YES

Dye: N719

TiO₂: 1 layer of DSL NR-AO (Dyesol)

Counter electrode: Platinum paste PT1 (Dyesol)

Active area: 0.88 cm²



Ageing:

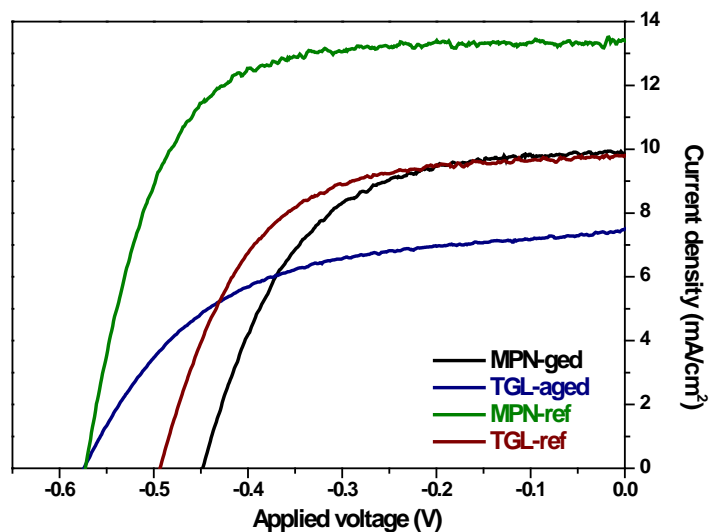
- 1) light soaking light soaking (0.8 sun) for 3000h at MPP →
- 2) then thermal ageing 85 °C dark (2000 h) @ ocp: Aged cells

No performance deterioration (reference or ref-cells)

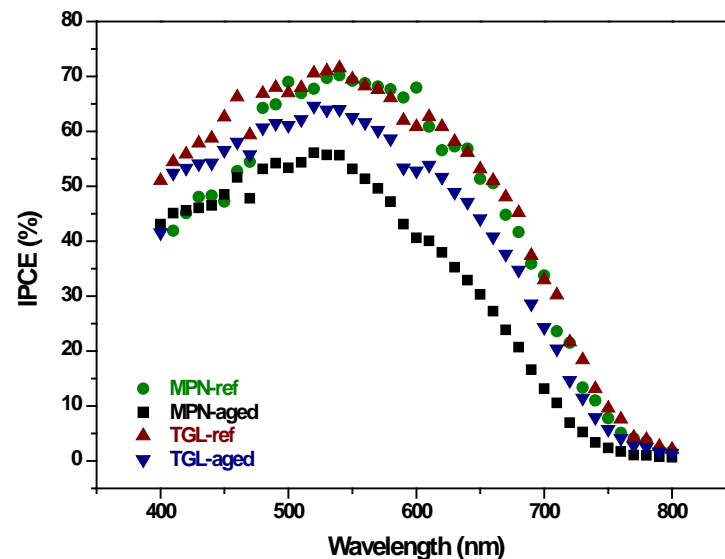
In-situ characterization: photoelectrochemistry (I-Vs, Impedance) + micro-Raman spectroscopy

Electrical characteristics @ 1 sun (AM1.5G)

J-V



IPCE



Electrolyte	J_{sc} (mAcm ⁻²)	V_{oc} (mV)	FF	η (%)
MPN-ref	13.4	566	0.67	5.1
MPN-aged	10.1	453	0.58	2.6
TGL-ref	9.8	496	0,59	2.8
TGL-aged	8.0	578	0.53	2.5

Conclusions (stability)

3000 h LS + 2000 h 85 °C dark with TGL-cells: test passed (10% efficiency loss)

The same aged (TGL) cells even give higher efficiencies under low light illumination conditions!!

MPN-cells loose the 50% of their initial performance: different degradation mechanisms

Both loose J_{sc} , FF. Different behavior in V_{oc}

Recombination is only slightly improved in both cells due to triiodide loss

V_{oc} seems to be determined by the E_c position

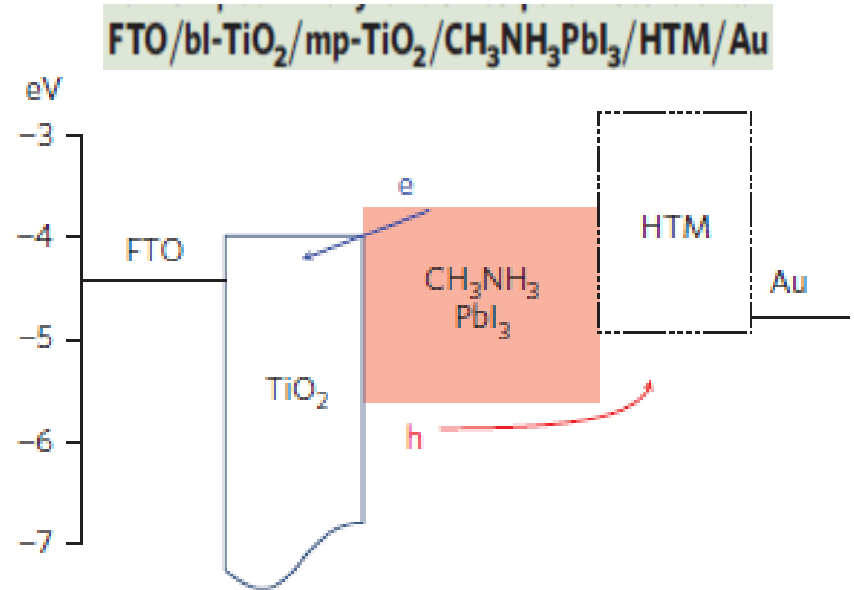
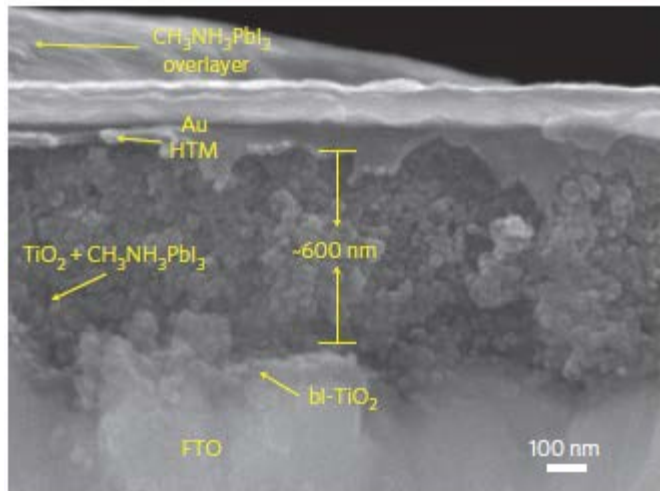
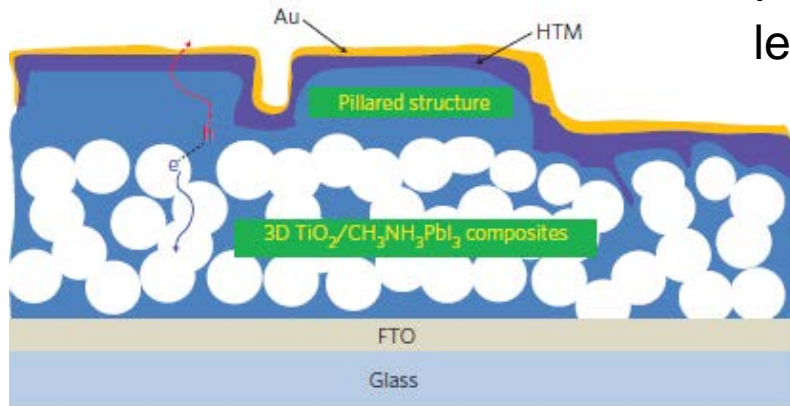
In MPN, a downward shift was observed, diminishing V_{oc}

Effects on the TGL-anode upon ageing, leading to an upward shift, increasing V_{oc} along with slight decrease of recombination (J_{sc} decrease). Regeneration efficiency decrease (due to -SCN loss in electrolyte-Raman detected)

Remaining problem: Better understand degradation effects; detect the species in MPN and TGL cells (dye extraction and chromatography)

Perovskites for new generation dye-sensitized solar cells

Perovskite nanoparticles (NPs) of methyl ammonium lead iodide ($\text{CH}_3\text{NH}_3\text{PbI}_3$) as light harvesters



HTM	J_{sc} (mA cm^{-2})	V_{oc} (V)	FF (%)	PCE, η (%)
P3HT	12.6	0.73	73.2	6.7
PCPDTBT	10.3	0.77	66.7	5.3
PCDTBT	10.5	0.92	43.7	4.2
PTAA	16.4	0.90	61.4	9.0
Without	6.8	0.68	53.8	2.5

Solid-state mesoscopic heterojunction solar cells

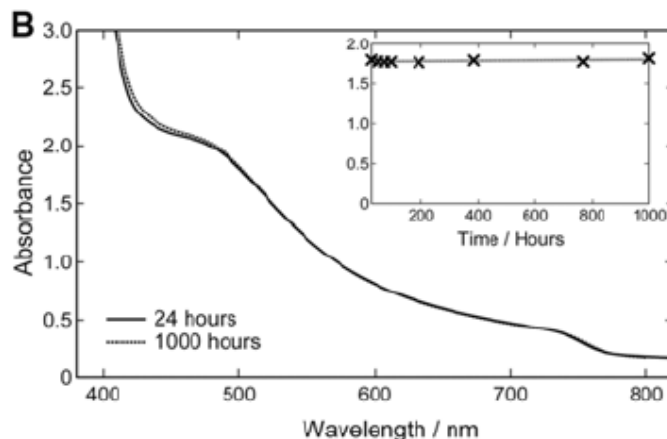
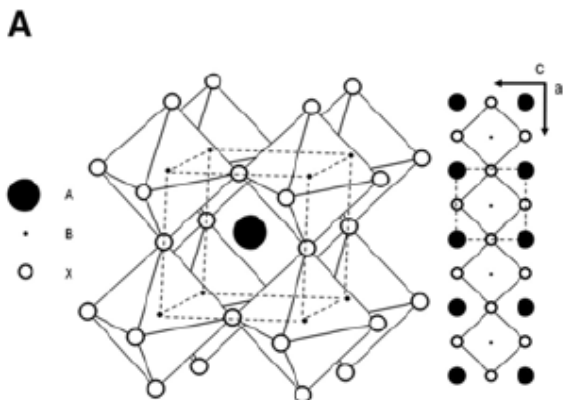
(HTM = poly-triarylamine): $J_{sc} = 16.5 \text{ mA}\cdot\text{cm}^{-2}$, $V_{oc} = 0.947 \text{ V}$, $ff = 0.727$, $PCE = 12\%$

M. Gratzel et al., 2013, Nature Photonics, DOI: 10.1038/NPHOTON.2013.80

M. Gratzel et al., SCIENTIFIC REPORTS | 2 : 591 , 2012, | DOI: 10.1038/srep00591

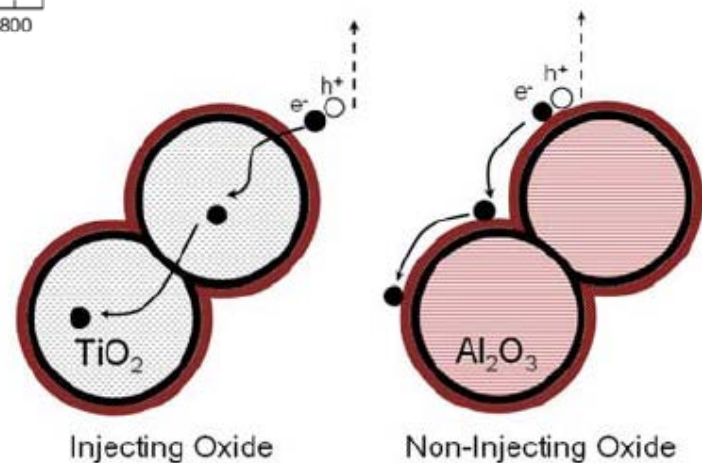
Perovskites for new generation dye-sensitized solar cells

methyl ammonium lead iodide chloride (CH_3NH_3) PbI_2Cl as light harvester



Optical bandgap: 1.55 eV

Mesostructured scaffold



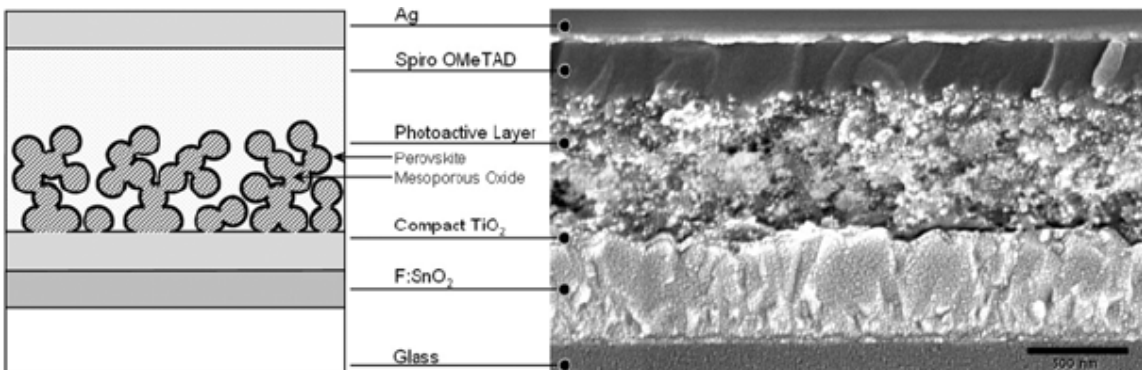
Stability?

using micro-Raman (NCSRD)

OXFORD

Meso-superstructured solar cell (MSSC): PCE=10.9%

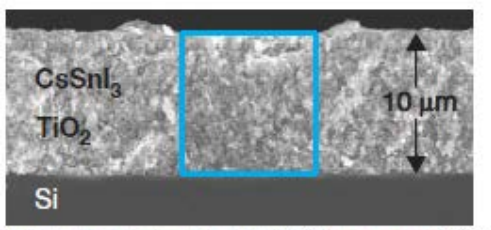
$\text{TiO}_2(\text{Al}_2\text{O}_3) / (\text{CH}_3\text{NH}_3)\text{PbI}_2\text{Cl} / \text{spiro-OMeTAD} / \text{Ag}$



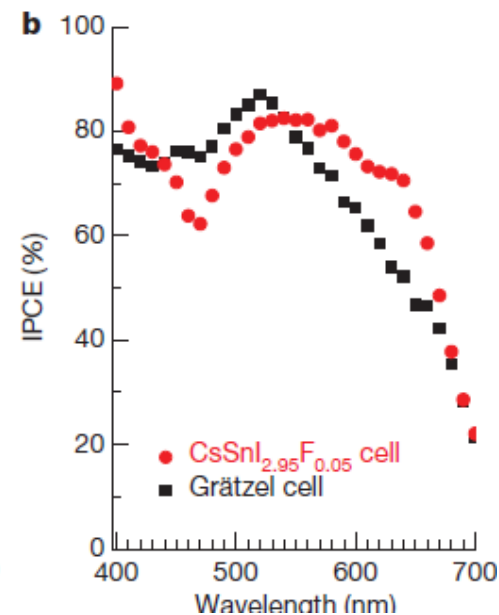
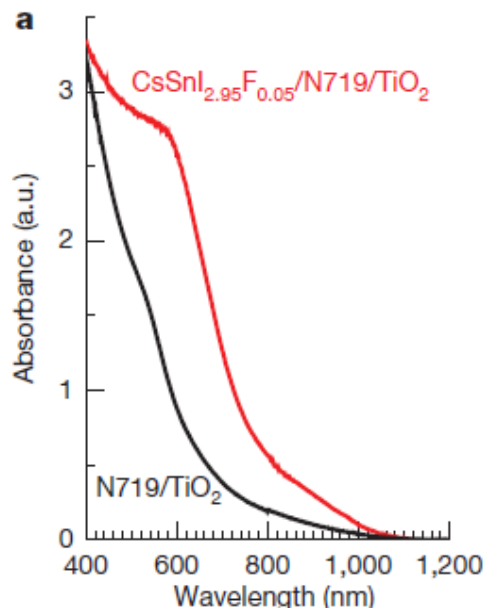
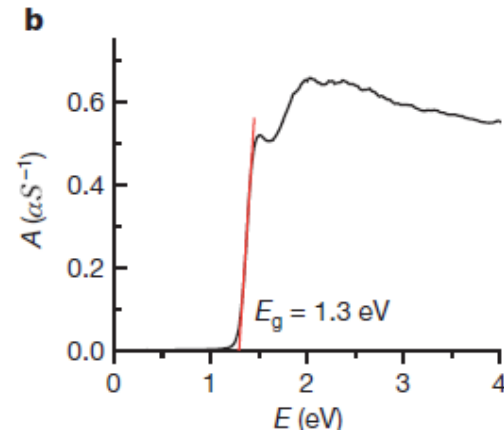
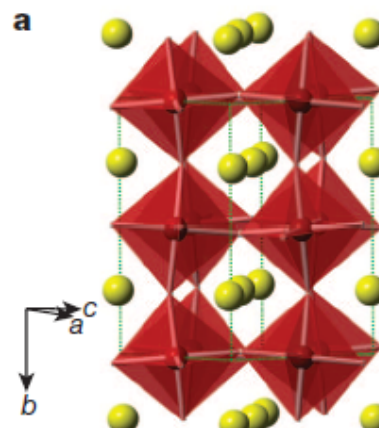
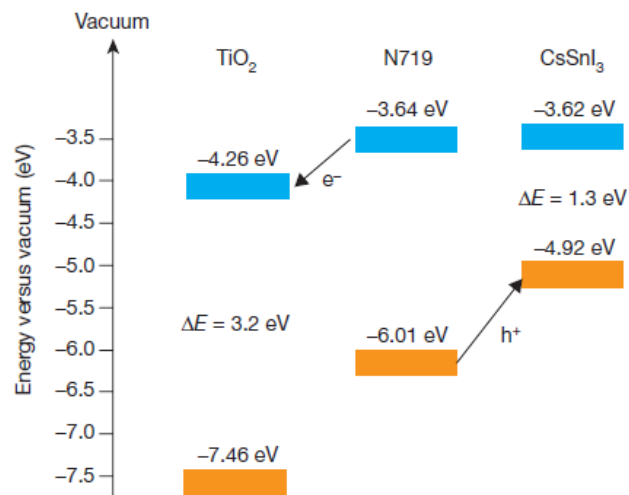
Perovskites for new generation dye-sensitized solar cells

CsSnI_3 p-type direct bandgap semiconductor, hole conductor (replacing electrolyte)

$\text{CsSnI}_{2.95}\text{F}_{0.05}/\text{N719 dye}/\text{TiO}_2$

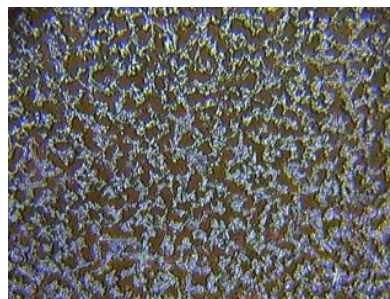
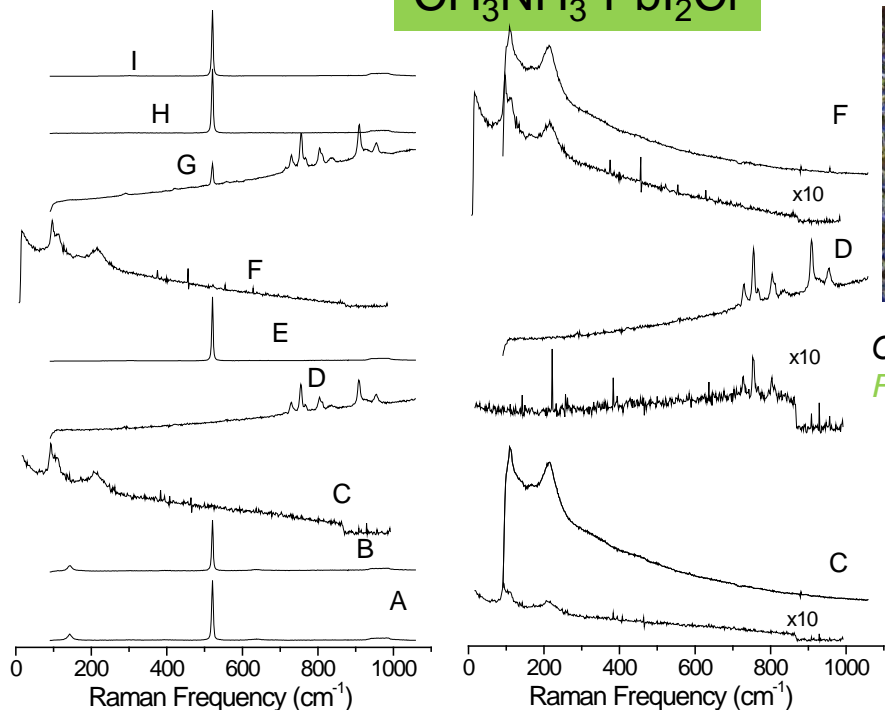


$J_{sc} = 19.2 \text{ mA}\cdot\text{cm}^{-2}$
 $V_{oc} = 0.732 \text{ mV}$
 $ff = 0.727$
 $\text{PCE} = 10.2\%$



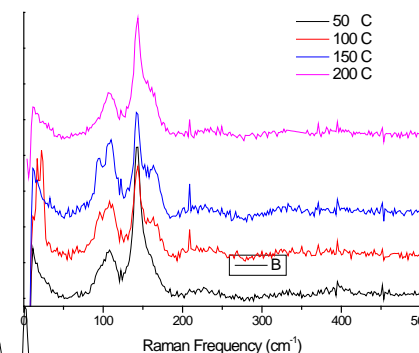
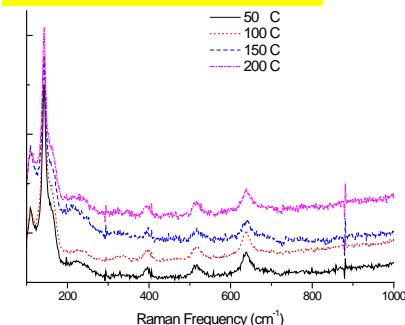
Raman work on Perovskites (materials and solar cells): preliminary data

CH₃NH₃-PbI₂Cl



Optical image 145x105 μm
F=Si/SiO₂+Al₂O₃+perovskite film

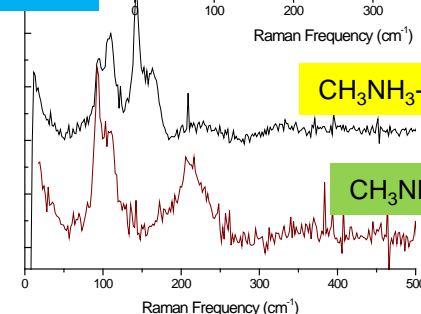
CH₃NH₃-PbI₃



NeXT filter

CH₃NH₃-PbI₃

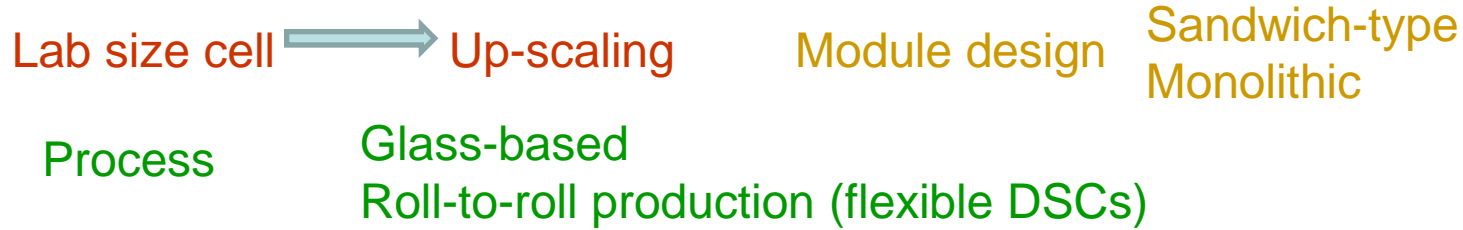
CH₃NH₃-PbI₂Cl



- A = Si/SiO₂ wafer + TiO₂ compact layer
- B = Si/SiO₂ wafer + TiO₂ compact layer + mesoporous Al₂O₃
- C = Si/SiO₂ wafer + TiO₂ compact layer + mesoporous Al₂O₃ + perovskite
- D = Si/SiO₂ wafer + TiO₂ compact layer + mesoporous Al₂O₃ + perovskite+spiro
- E = Si/SiO₂ wafer + mesoporous Al₂O₃
- F = Si/SiO₂ wafer + mesoporous Al₂O₃ + perovskite
- G = Si/SiO₂ wafer + mesoporous Al₂O₃ + spiro
- H = Si/SiO₂ wafer
- I = Si/SiO₂ wafer + low-temperature processed TiO₂ compact layer

- Strong Photoluminescence (PL) background
- Response very sensitive to the laser power
- Annealing (50, 100, 150, 200 °C): influence on the Raman spectrum
- Light stress (1 sun, AM 1.5 G, without UV filter, from 10-120 min): crystallization
- Perovskite crystal lattice vibrations (10-100 cm⁻¹)

Module development



Modules	Size (cm ²)	η (%)
Pecell Technologies, Inc., Japan	900	3.5
Sharp corporation, Japan	625	
Institute of Plasma Physics, China	900	5.9
Fraunhofer ISE, Germany	3600	3
Toyota, Japan,	90	
Sony, Japan (module efficiency record)		9.2

Demonstration activities (> 1m²)

G24i, Wales

Institute of Plasma Physics, China

3G Solar Ltd, Israel

Toyota, Japan

Dyesol Ltd, Australia

Applications

Mobile electronics, G24i

Flexible SCs on metal, Corus

SCs on plastic, Konarka

BPIV, Pilkington

Industrialization

Industrialization policy

- demonstration projects/prototypes development
- greater commitment of resources at the project level
- sharpening of focus on providing next generation technology
- reduction in costs associated with new business development
- addressing the multiple commercial opportunities for the global PV market place

Industrialization key players

- Investors and analysts seeking real data on DSC
- Manufacturers considering including DSC in their product ranges
- Case studies of companies already in the field
- Product designers and architects to gain insight into the real advantages of DSC compared to classical photovoltaics
- Researchers to gain an understanding of the key industrial criteria to enable better direction of R&D
- Students to benefit from a holistic overview of all aspects of DSC

IPRs

Patent portfolio

DSC-IC 2006 in Canberra/Australia

1st DSC Industrialization Conference



Held in Australia's capital city, Canberra, on February 9 and 10 the Conference was attended by more than 70 international scientists, architects, entrepreneurs and industrialists.

Attendees at the world's first conference to discuss 'Industrialisation of DSC: from Research to Product' shared a great deal of information and renewed motivation in their programs to research and industrialise the technology and its applications.

<http://www.dyesol.com/index.php?element=Newsletter2>

DSC-IC 2007 in St Gallen/Switzerland

The 2nd DSC Industrialisation Conference (September 2007-St Gallen Switzerland) attracted attendees from 25 countries with an even mix of industrial and academic delegates (> 250 participants).

Dyesol's Conference stand



Application of DSC to a real building construction



Top academic, institutional, government and industry experts in DSC technology from around the world delivering presentations

Participation of over 200 delegates in the field of DSC, amongst other leading personalities from research institutions and CEO's from the world's leading PV companies

<http://www.dyesol.com/conference09/index.php?element=Conference+Programme>



DSC-IC 2010 in Colorado Springs, USA, from November 1st to 4th 2010

Over 30 speakers who are experts in developing and commercialising DSC technology

Excellent networking opportunities with over [200 attendees](#).

Comprehensive coverage of market developments, emerging applications and advances in DSC technology

Poster session with presenters from leading companies and research institutes active in DSC development

<http://www.dsc-ic.com>

Conclusions (industrialization)

- 100 research groups working in DSC research around the world
Switzerland, the Netherlands, the UK, Spain, Germany, Sweden, Finland, Portugal, China, Japan, South Korea, Australia, New Zealand, South Africa and the USA
- Energy conversion efficiency
- Long-term stability, particularly at high temperatures
- Endurance tests under light soaking
- Research and development (clustering, technology transfer)
- Materials
- Devices efficiency and stability
- IPRs-Patents portfolio
- Prototypes (modules)
- Scale up (materials, processes and devices)
- Demonstration projects
- Market exploitation: manufacture, commercialization (intention to commercialize)

In the end it will be the positive combination of efficiency and stability which will determine the commercial success of DSCs

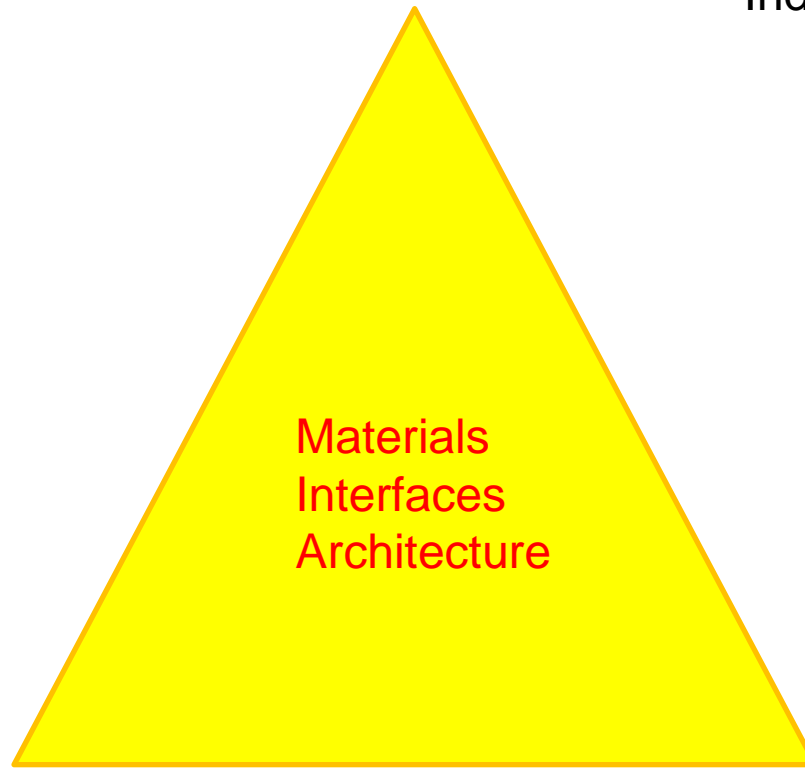
DSCs technological success ?

Increase light harvesting efficiency
Reduce charge recombination
Optimize electron transport and collection
Improve hole transport in the electrolyte
Manage incident light

←← main limitations

Performance Efficiency

Lab: 15%
Industry: 10%



Scale up
Demonstration
Industrialization

Emerging and new applications call for:

- colour
- flexibility
- light weight
- easy integration
- ... further development

Cost
<math><0.5 \text{ € / Wp}</math>

Stability ?



Acknowledgements

-NCSRDR

- Dr. Athanasios G. Kontos
- Dr. Thomas Stergiopoulos
- Dr. Vlassis Likodimos
- Dr. G. Vougioukalakis
- Dr. M. Konstantakou
- Naoumis Vaenas
- Maria Bidikoudi
- Dorothea Perganti

-External collaborators

- | | |
|----------------------|-------------------|
| Prof. P. Lianos | Patras, Greece |
| Prof. Patrik Schmuki | Erlangen, Germany |
| Dr. Henry Snaith, | Oxford, UK |
| Dr. Gavin Tulloch | |
| Dr. Hans Desilvestro | Dyesol, Australia |
| Dr. Damion Milliken | |



Funding



- a) FP6 STREP (NMP-CT-2006-033313) : Ti-Nanotubes-Preparation, Characterization and Application of Self-Organized Titanium Oxide-Nanotubes (**Ti-Nanotubes**)
- b) FP7-ENV-NMP-2009-SMALL-3: Sensitizer Activated Nanostructured Solar Cells (**SANS**)
- c) FP7-Marie-Curie ITN-316494: Dye Sensitized Solar Cells of Enhanced Stability (**DESTINY**)
- d) GSRT/Ministry of Development-Greece **ARISTEIA (AdMatDSC-1847), THALES**

DSC Companies

- Dyesol: new manufacturing facilities in Queanbeyan on the 7th of October 2008.
- Solaronix, a Swiss company specialized in the production of DSC materials since 1993, has extended their premises in 2010 to host a manufacturing pilot line of DSC modules.
- SolarPrint founded in 2008 by Dr. Mazhar Bari, Andre Fernon and Roy Horgan. SolarPrint is the first Ireland-based commercial entity involved in the manufacturing of PV technology. SolarPrint's innovation is the solution to the solvent based electrolyte which to date has prohibited the mass commercialisation of DSSC.
- G24innovations founded in 2006, based in Cardiff, South Wales, UK. On October 17, 2007, claimed the production of the first commercial grade dye sensitized thin films. G24i now purchase all of their DSC Dye's from Dyesol.
- Hydrogen Solar is another company making dye-sensitized cells.
- Sony Corporation has developed dye-sensitized solar cells with an energy conversion efficiency of 10%, a level seen as necessary for commercial use. Sony is now being supplied materials by Australia's Dyesol.
- 3G Solar, Israel

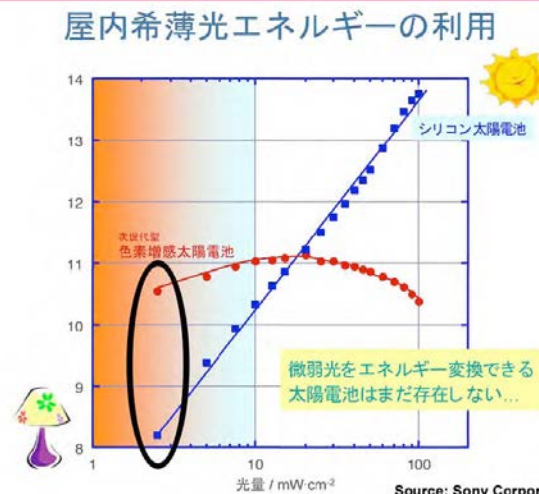
Advantages of DSCs vs. Silicon Cells

- Low cost and ease of production
- Performance increases with temperature narrowing the efficiency gap
- Bifacial configuration - advantage for diffuse light and albedo
- Efficiency less sensitive to angle of incidence
- Transparency for power windows
- Color can be varied by selection of the dye, invisible PV-cells based on near-IR sensitizers are feasible
- Low energy content (for silicon this is 5 GJ/m² !), payback time is only a few months as compared to years for silicon.
- Outperforms amorphous Si

Emerging and new applications call for:

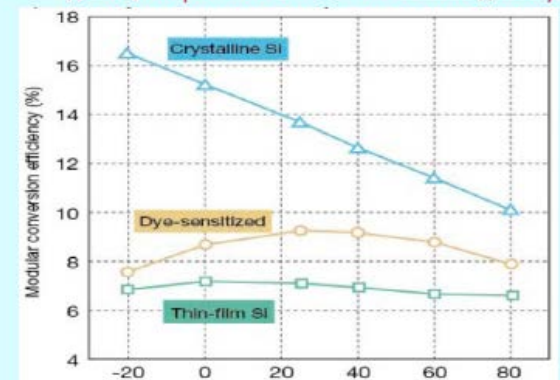
- colour
- flexibility
- light weight
- easy of integration
- ... further development

Dye sensitized solar cells outperform silicon at lower light levels



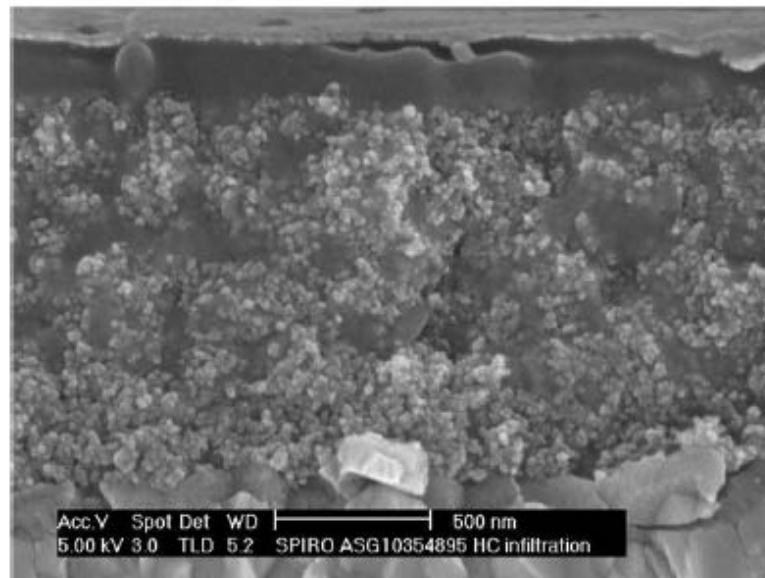
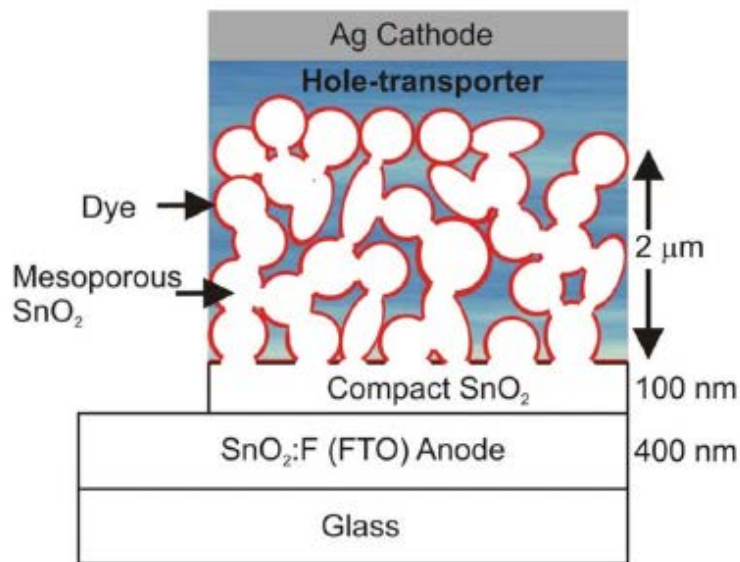
Dye sensitized solar cells deliver high overall performance

Effect of temperature on module conversion efficiency

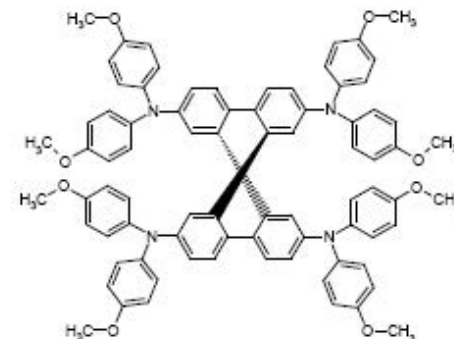


Source: Tetsuo Nozawa, Nikkel Electronics Asia (July 2008), Data from Sony

Optimization of electrolyte-hole transport medium



- New quasi-solid-state and ionic liquid electrolytes
- Improve performance of solid-state hole-transporters – pore filling and new formulation of ionic additives



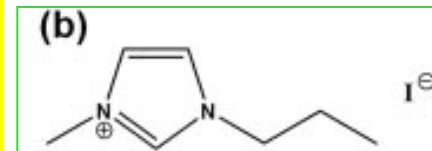
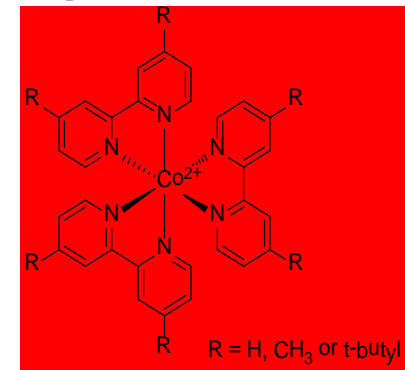
INDUSTRIAL RESEARCH OBJECTIVES for DSCs

- **A new generation** of nanostructured molecular **photovoltaics**
- **Reliable and affordable solar electricity**
- **Long term stability** and **low embodied energy**

Current research directions (laboratory level)

Enhanced light harvesting and conversion by using:

- **Advanced meso-structures**
- **New sensitizers**
- **New redox mediators**
- **Solid state heterojunctions**
- **Quantum dot injection cells**
- **Tandem devices**
- **New solid nanocomposite electrolytes (ionic liquids)**
- **Perovskites**



Stability: where we are at the moment

- No specific testing protocol for DSCs
- Typical light soaking and thermal ageing tests:
 1. Light soaking 1000 h (0.8-1 sun) @ 60 °C
 - ✓ various electrolytes (MPN, butyronitrile and ILs)
 - ✓ dyes (Ru²⁺- based complexes and organic dyes)

Dyesol: only 17 % efficiency loss > 25000 h

2. Thermal ageing: (usually) dark @ 55-85 °C
 - ✓ only some electrolytes and dyes
3. Thermal cycling: -40°C to +85 °C
 - ✓ [R. Harikusun et al., Solar Energy 85 (2011) 1179]

International Standards for **crystalline silicon** and **thin film** PV devices

Overview of IEC 61215 / IEC 61646 tests

Code	Qualification Test	Test Conditions
10.1	Visual Inspection	according defined inspection list
10.2	Maximum Power Determination	measurement according to IEC 60904
10.3	Insulation Test	1000 VDC + twice the open circuit voltage of the system at STC for 1 min, isolation resistance * module area > 40 MΩ·m ² at 500 VDC
10.4	Measurement of Temperature Coefficients	Determination of the temperature coefficients of short circuit current, open circuit voltage and maximum power in a 30°C interval
10.5	Measurement of NOCT	total solar irradiance = 800 W/m ² wind speed = 1 m/s
10.6	Performance at STC and NOCT	cell temperature = NOCT / 25°C irradiance = 800 W/m ² / 1000 E/m ² measurement according to IEC 60904
10.7	Performance at low Irradiance	cell temperature = 25°C irradiance = 200 W/m ² measurement according to IEC 60904
10.8	Outdoor Exposure Test	60 kWh/m ² solar irradiation
10.9	Hot-Spot Endurance Test	5 hour exposure to > 700 W/m ² irradiance in worst-case hot-spot condition
10.10	UV-preconditioning test	15 kWh/m ² UV-radiation (280 - 385 nm) with 5 kWh/m ² UV-radiation (280 - 320 nm) at 60°C module temperature
10.10*	UV-Exposure according IEC 61345	Min. 15 kWh/m ² UV-radiation (280 - 400 nm) with 7.5 kWh/m ² UV-radiation (280 - 320 nm) at 60°C module temperature
10.11	Thermal Cycling	50 and 200 cycles -40°C to +85°C
10.12	Humidity Freeze Test	10 cycles -40°C to +85°C, 85% RH
10.13	Damp Heat	1000 h at +85°C, 85% RH
10.14	Robustness of Terminations	As in IEC 60068-2-21
10.15	Wet Leakage Test	Evaluation of insulation of the module under wet conditions
10.16	Mechanical Load Test	Three cycles of 2400 Pa uniform load, applied for 1 h to front and back surfaces in turn
10.17	Hail Test	25 mm diameter ice ball at 23 m/s, directed at 11 impact locations
10.18	Bypass diode thermal test	Asses adequacy of thermal design of bypass diodes at a current of 1.25 x Isc running through the diodes at module temperature of 75°C
10.19**	Light soaking	Light exposure of cycles of at least 43 kWh/m ² and module temperature of 50°C ± 10 °C, until Pmax is stable within 2 %

* Tests can alternatively be used

** Tests only relevant for IEC 61646 qualification

Thermal stability: a mini-review

Systems that pass the 80 °C test:

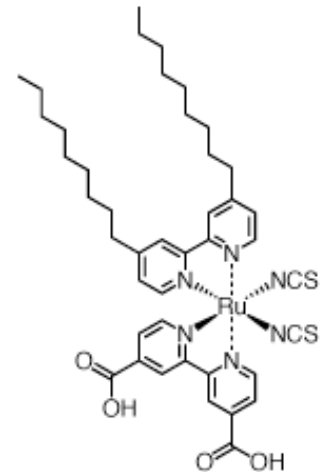
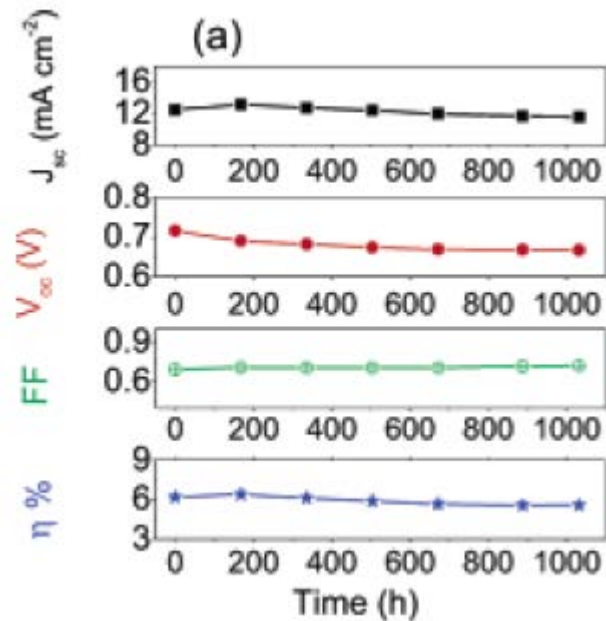
- Hydrophobic dyes such as Z907
- Ionic liquid electrolytes

[P. Wang et al. JACS 127 (2005) 808]

- Gel electrolytes

[W. Kubo et al. Chem. Commun. 2002, 374]

[P. Wang et al. Nat. Mater. 2 (2003) 402]



[P. Wang et al. JACS 128 (2006) 7732]

- 1 striking result (only 24% relative loss) at 85 °C under 1 sun illumination

[J. Goldstein et al. Sol. Energ. Mater. Sol. C. 94 (2010) 638]

Motivation to continue work

- Extend thermal ageing testing at 85 °C (and increase ageing time)

Ageing at higher temperatures (>60 °C) could accelerate degradation or even create new paths for degradation. The group of M. Grätzel have seen significant differences between 60 and 80 °C

[J. Ho Yum et al., Nanotoday 5 (2010) 91]

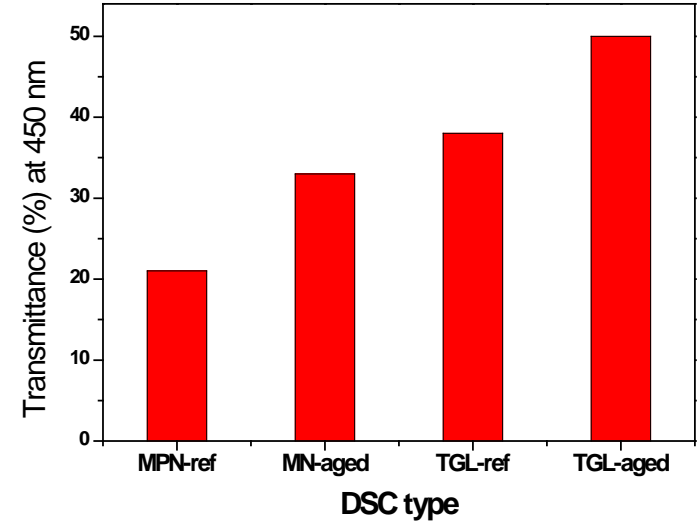
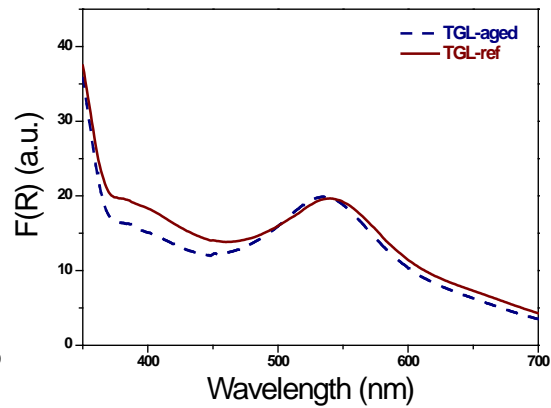
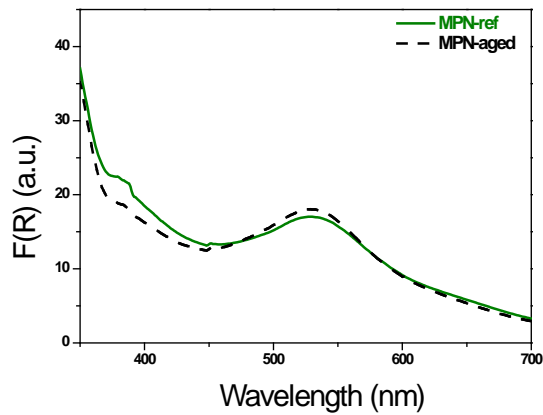
Temperatures of 85 °C could be reached in tropical locations

[H. Desilvestro et al. "Packaging, scale-up and commercialization of dye solar cells", CRC Press, 2010]

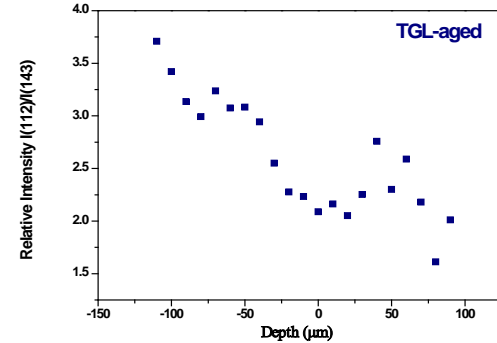
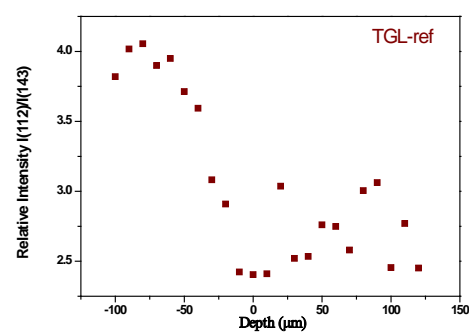
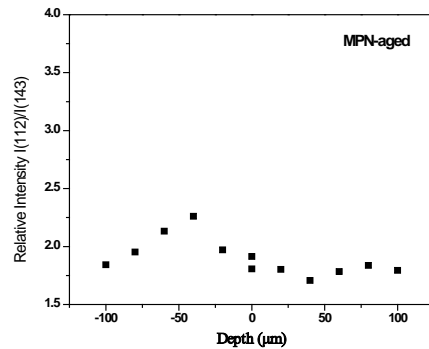
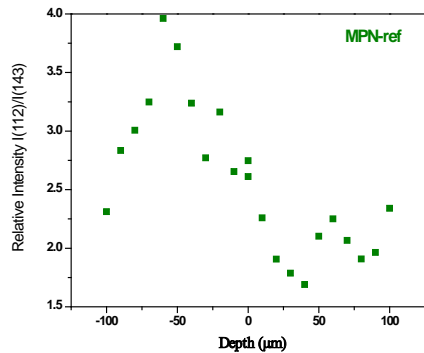
- Test improved sealing of devices (secondary sealing assures O₂ and H₂O ingress and protects the cells from electrolyte leakage-triiodide loss)

Triiodide loss detection

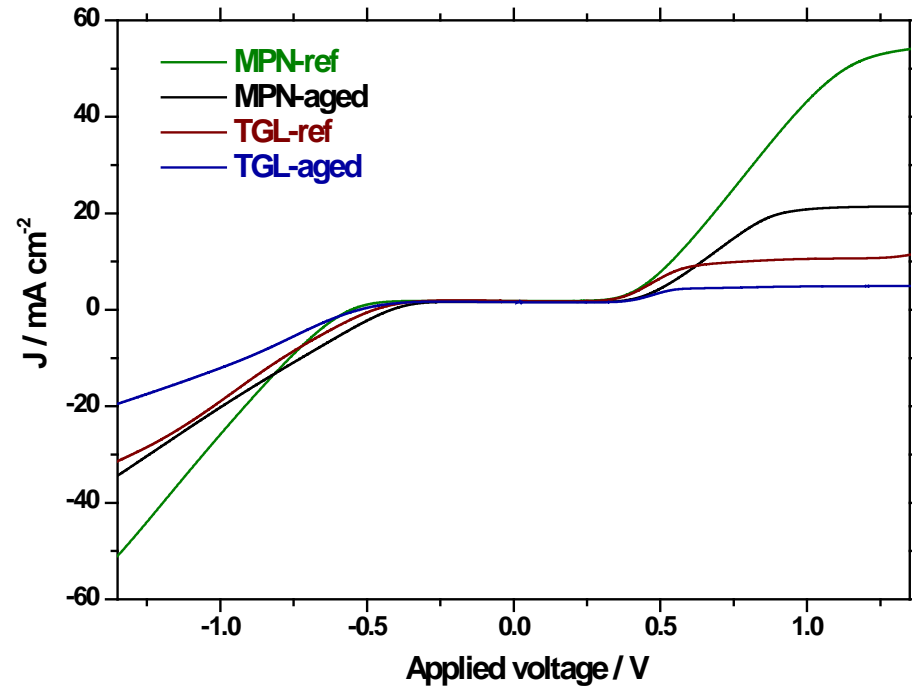
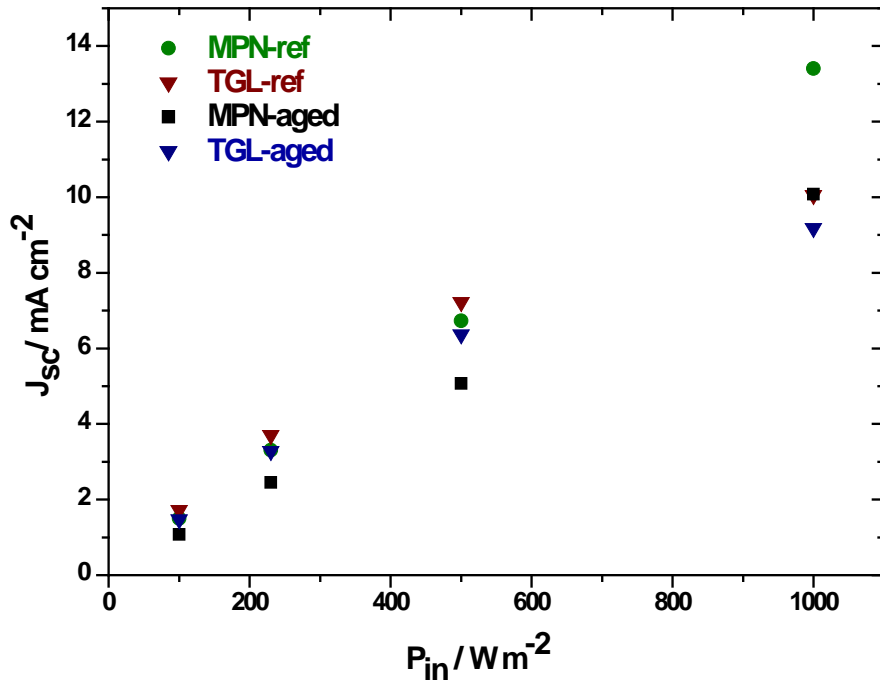
Optical:



Raman:



J_{sc} limitations?



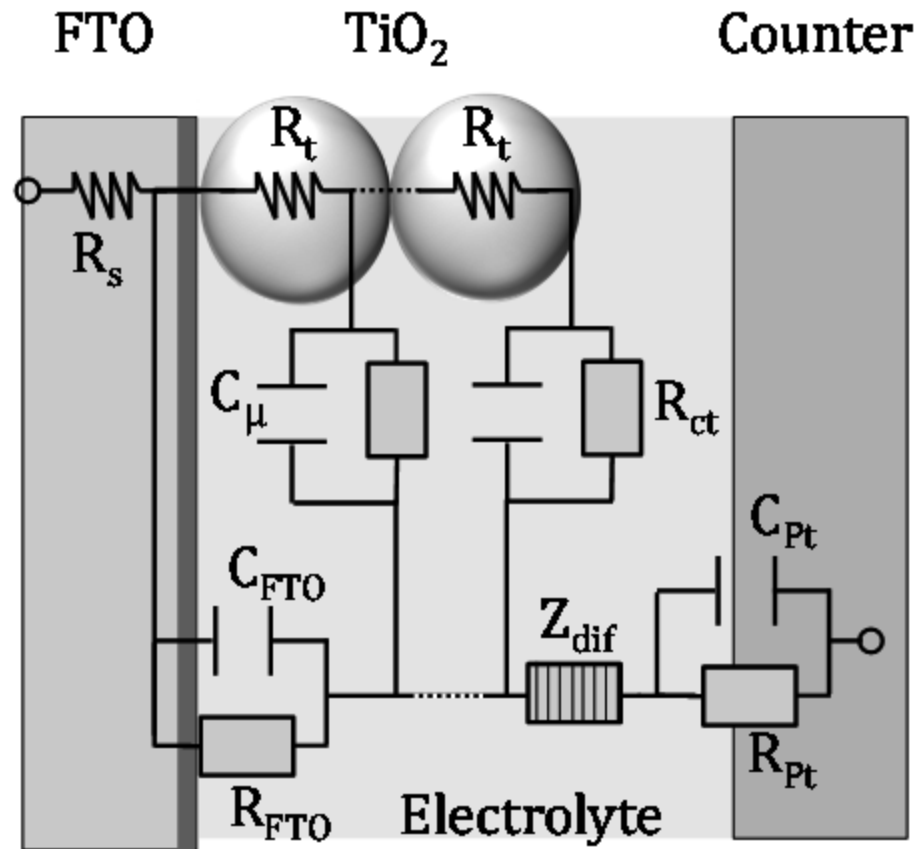
- $J_{DL} > 10 \text{ mA/cm}^2$ for all cells except for TGL-aged cells
- Linearity preserved for MPN cells; issues with the TGL cells

Performance under low light illumination conditions

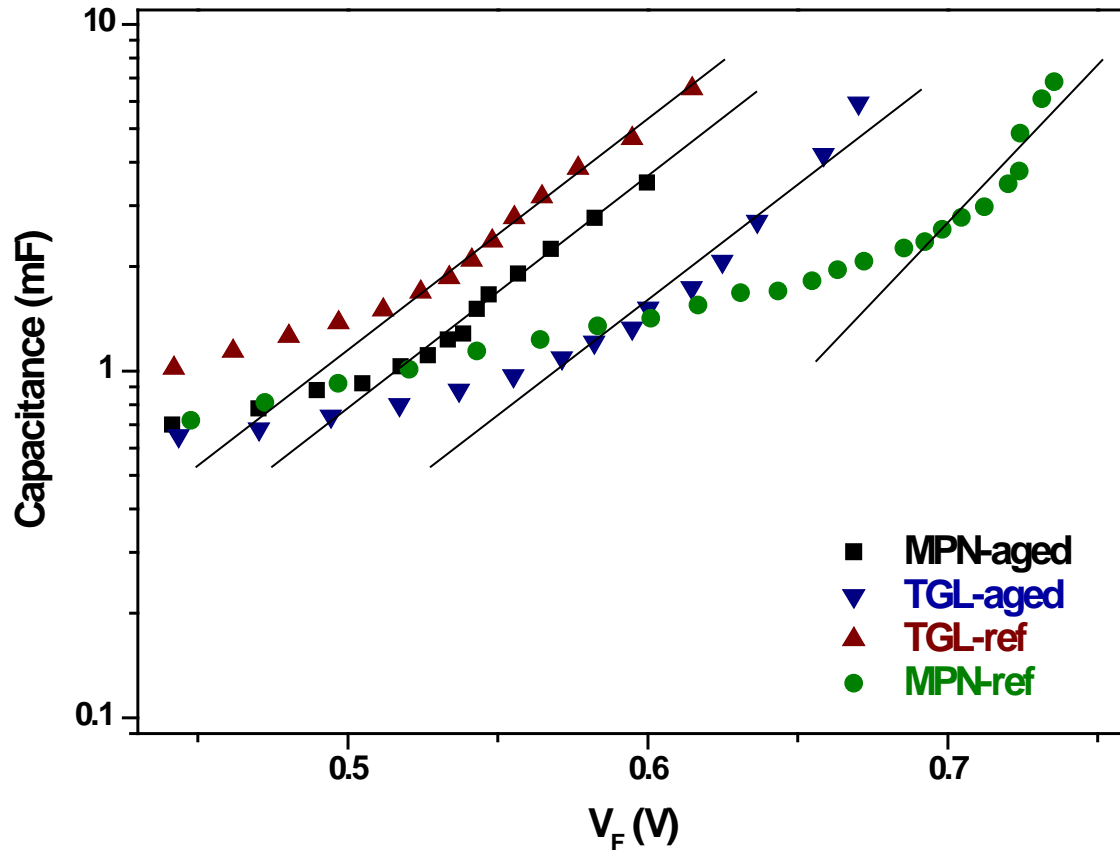
I-Vs under 0.1 sun

Electrolyte	J_{sc} (mAcm ⁻²)	V_{oc} (mV)	FF	η (%)
MPN-ref	1.50	492	0.66	4.85
MPN-aged	1.08	380	0.65	2.65
TGL-ref	1.72	435	0.65	4.83
TGL-aged	1.47	508	0.67	5.03

EIS: DSC equivalent circuit



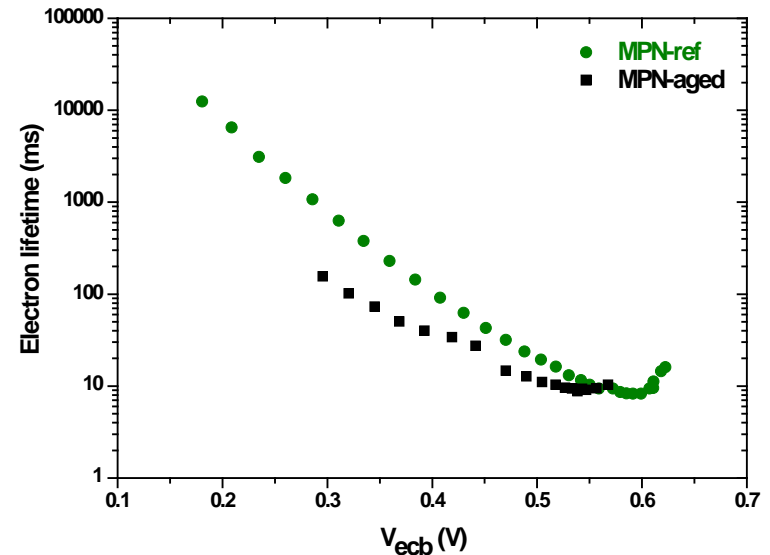
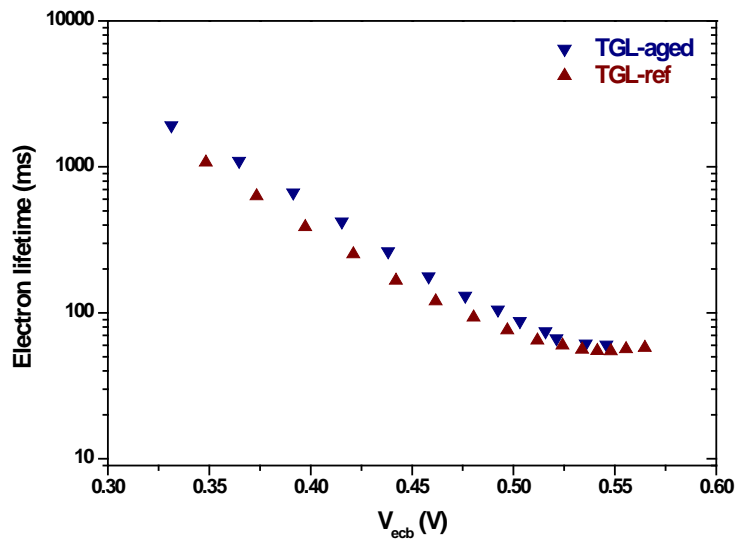
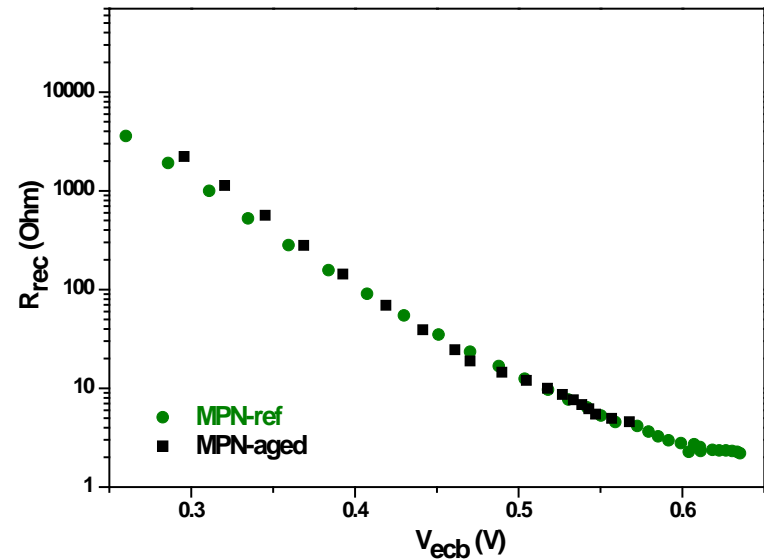
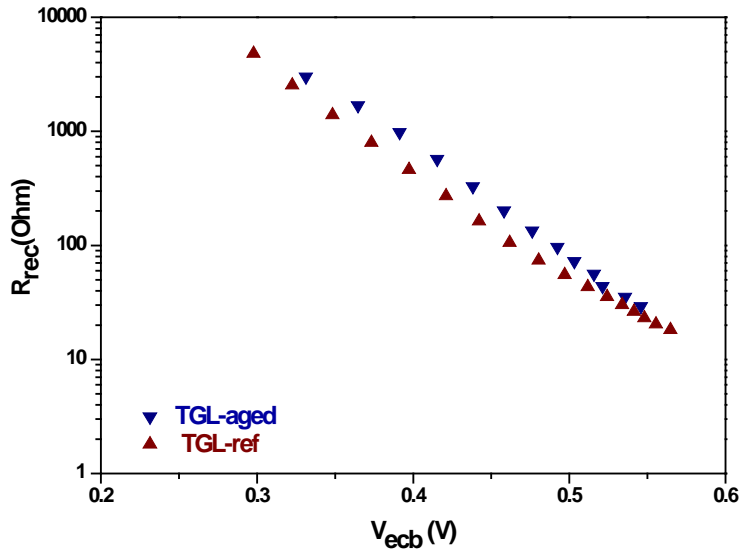
TiO₂/electrolyte capacitance



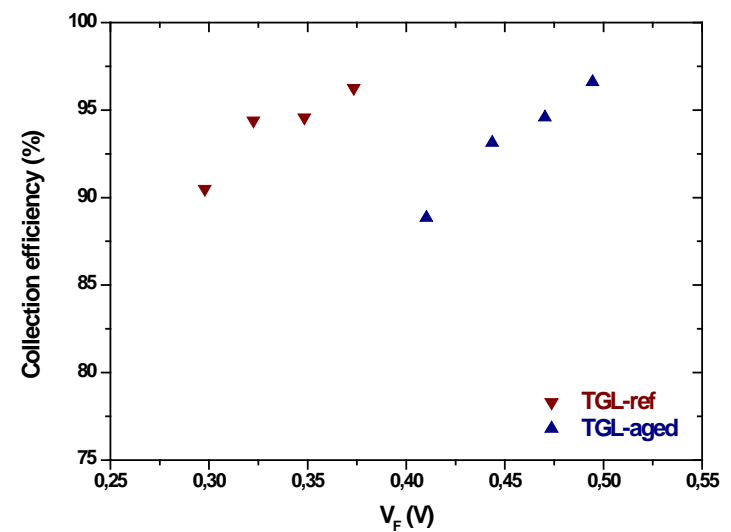
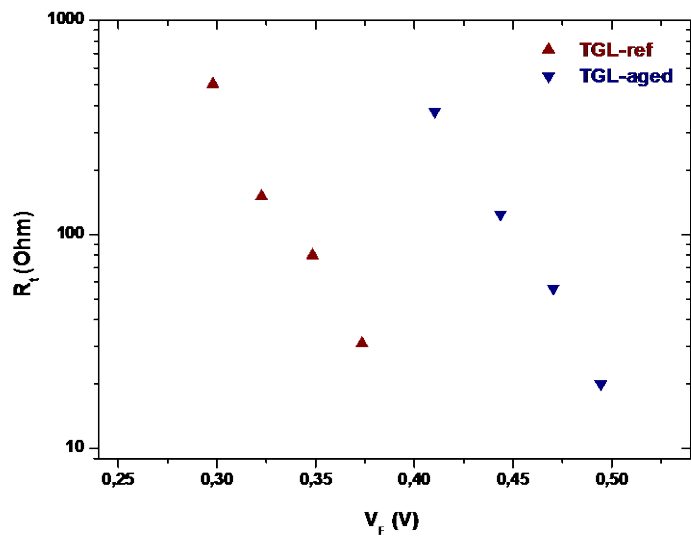
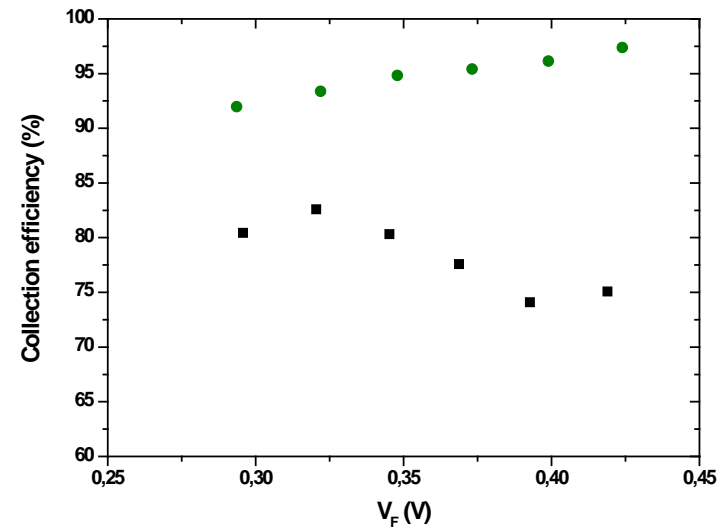
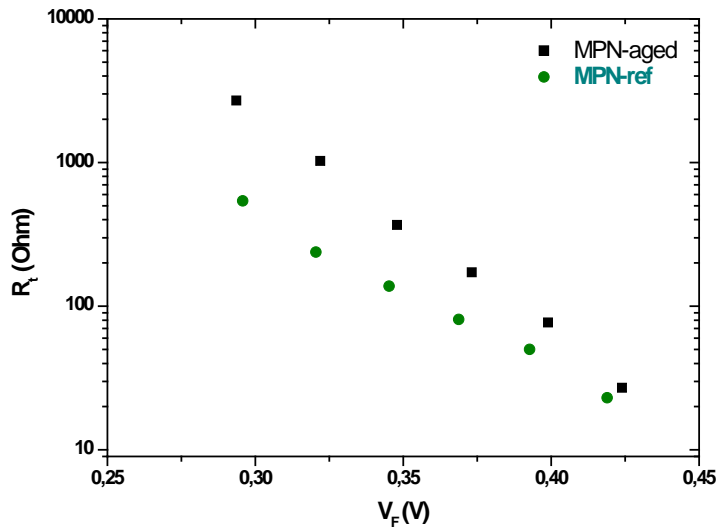
$$C_{\mu} = C_0 \exp\left[\frac{qV_F}{kT_0}\right]$$

$$C_0 = \frac{(1-p)Lq^2N_L}{kT_0} \exp\left[\frac{q(E_{F0} - E_c)}{kT_0}\right]$$

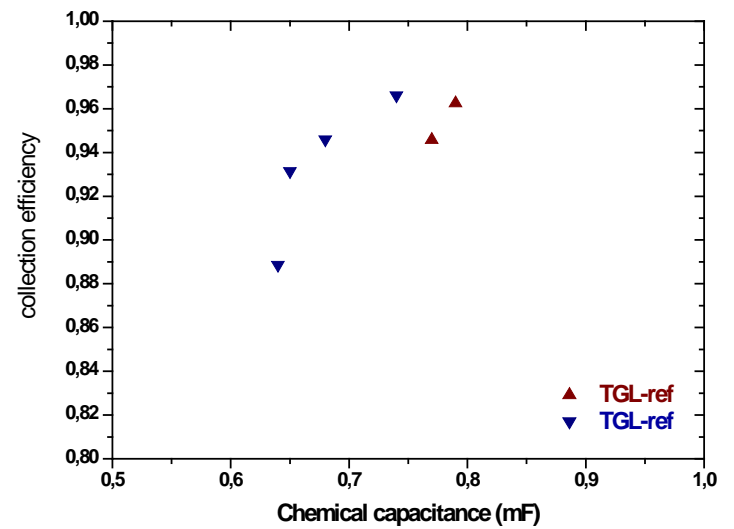
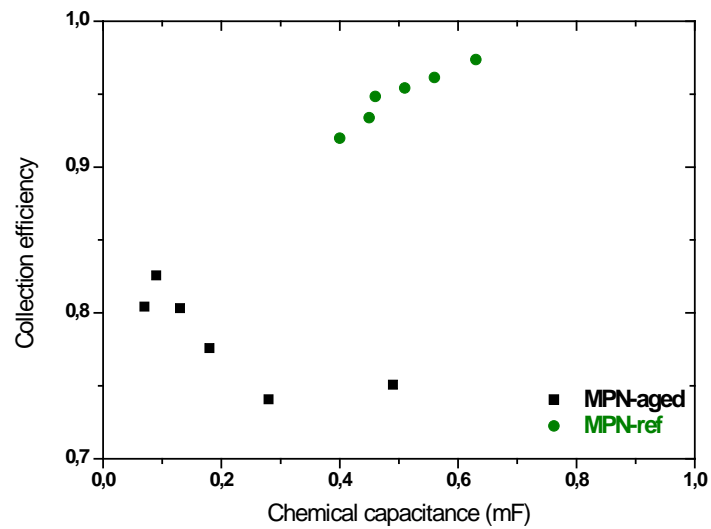
Recombination dynamics



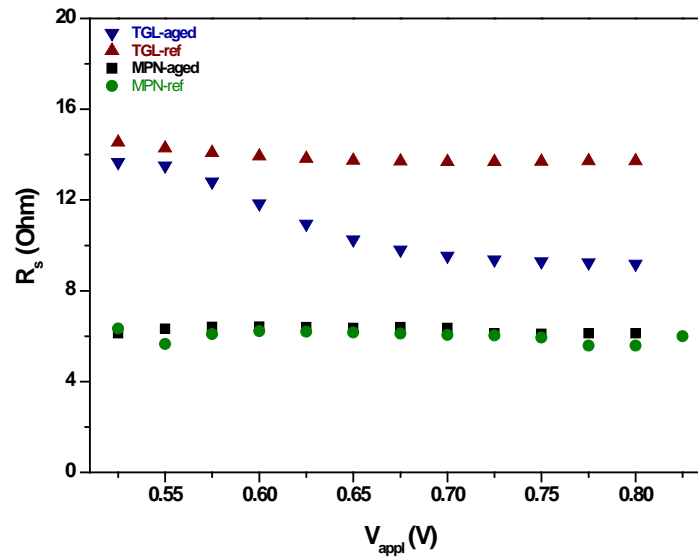
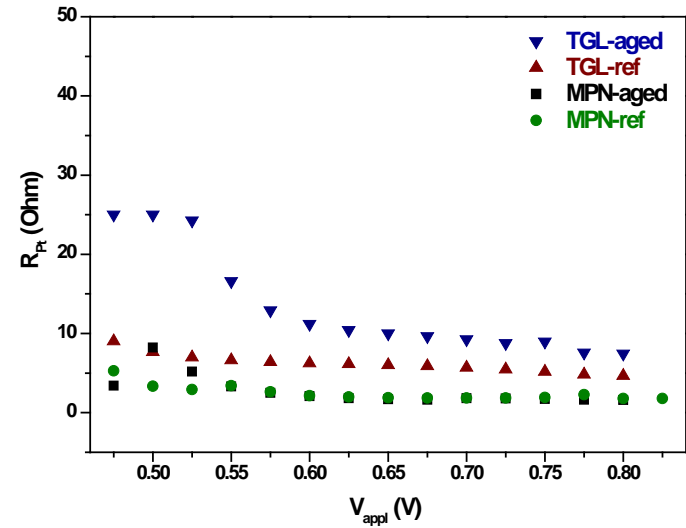
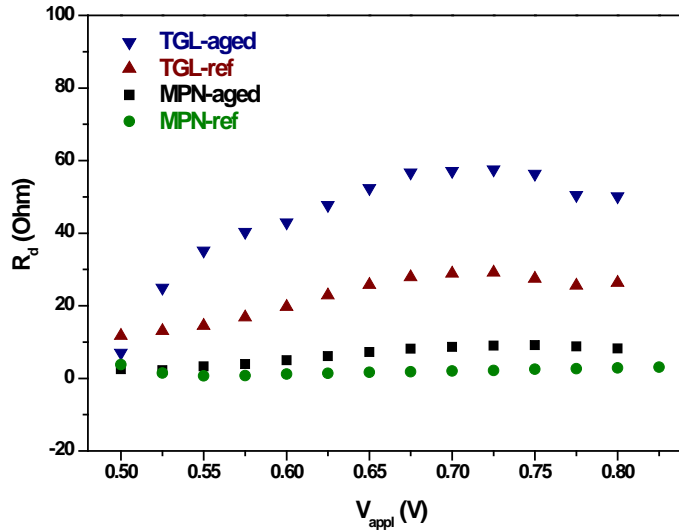
Transport resistance – Collection efficiency



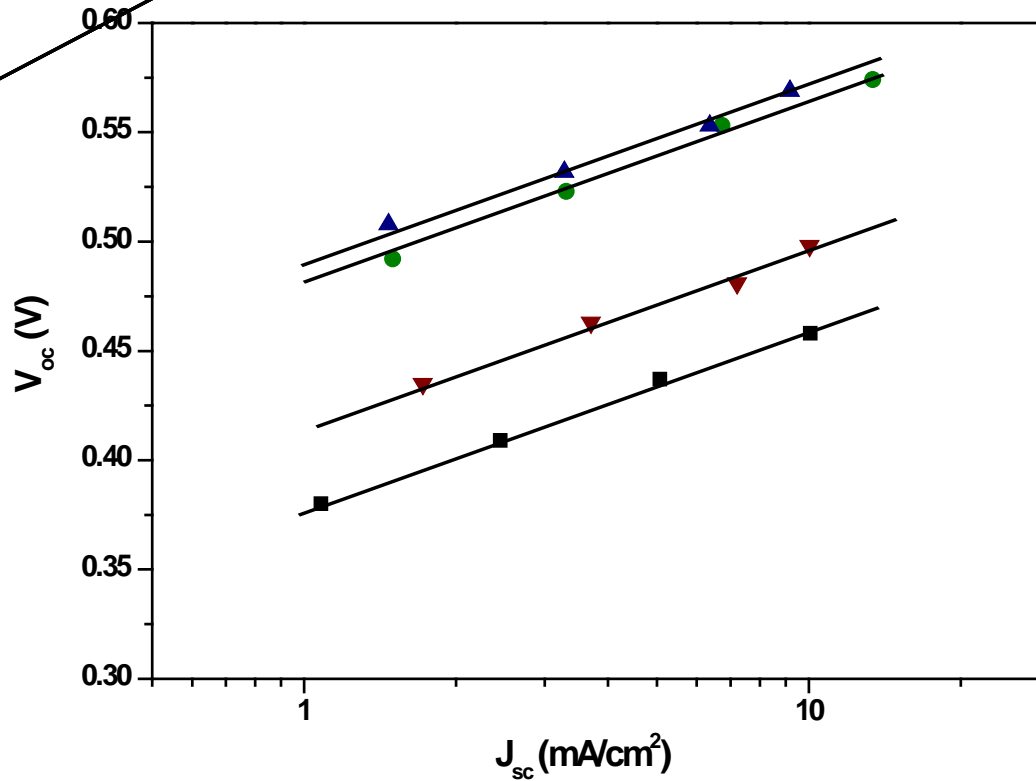
Collection efficiency @ identical DOS



Ohmic or pseudo-ohmic resistances

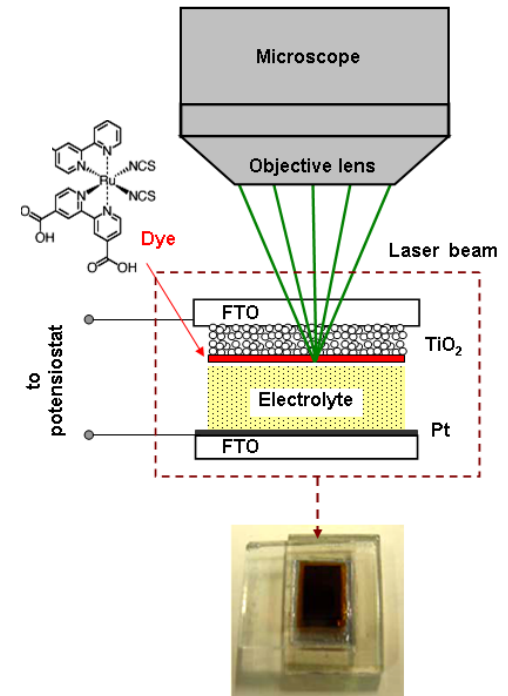
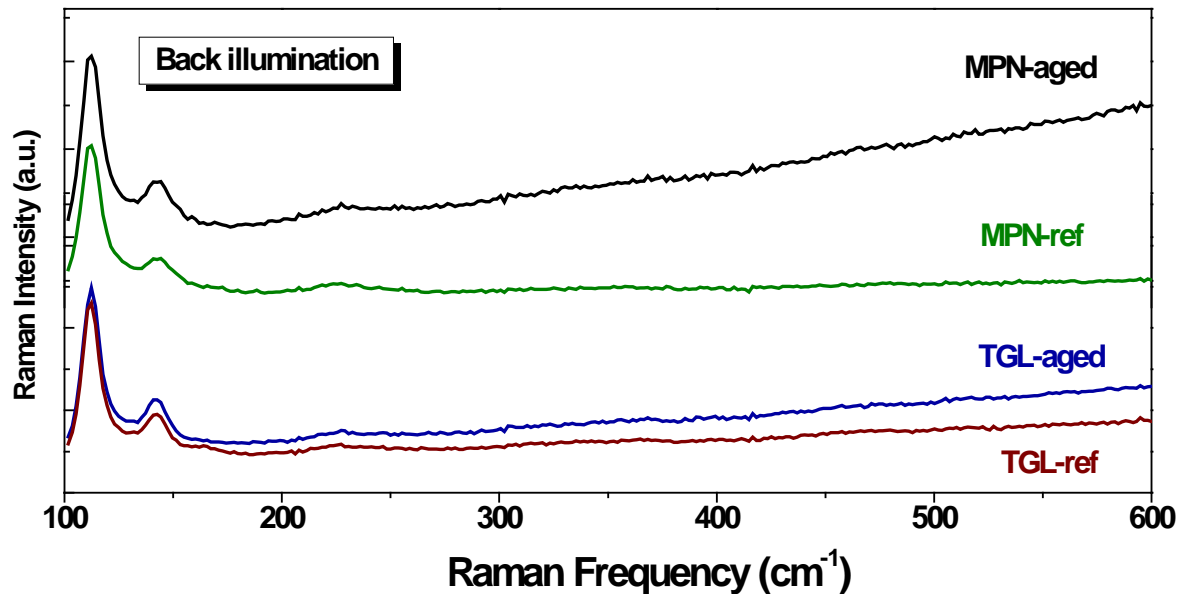


V_{oc} dependence on J_{sc}



Dye	mV per decade	m	1/m
MPN-ref	83	1.41	0.71
MPN-aged	72	1.22	0.82
TGL-ref	81	1.37	0.73
TGL-aged	82	1.39	0.72

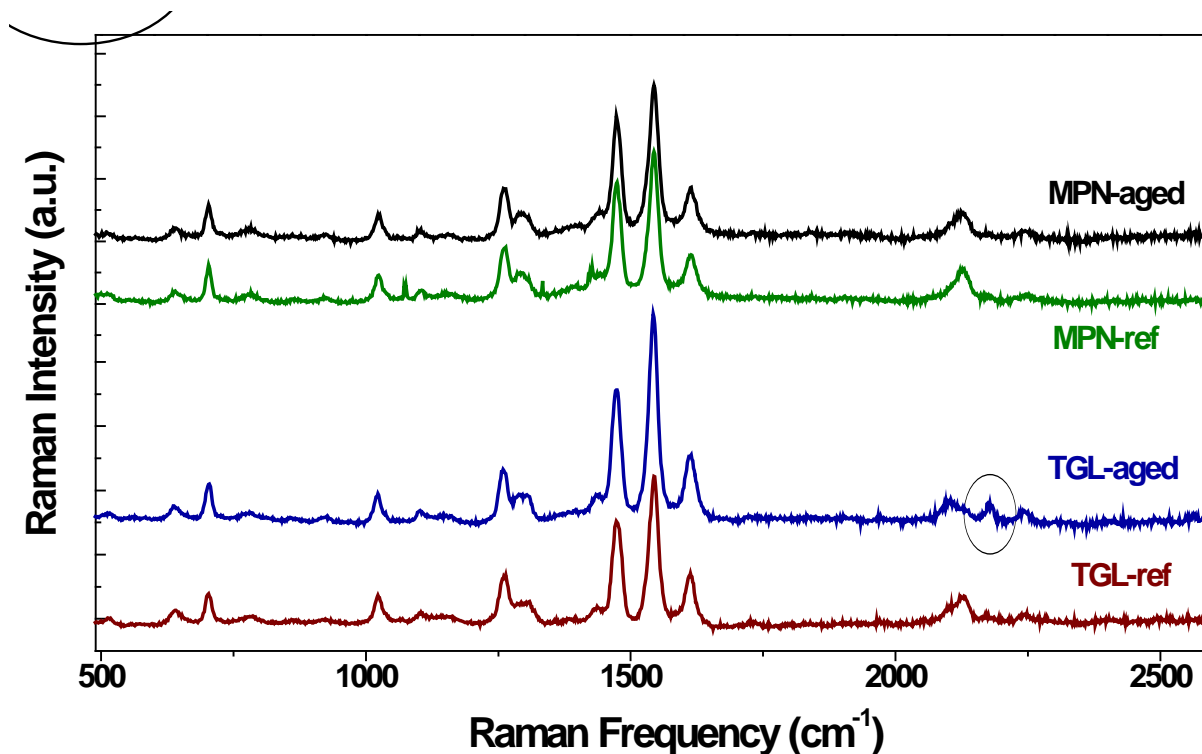
Micro-Raman spectroscopy



MPN aged cells: Strong background luminescence probably due to species formed in the electrolyte [*N. Kato et al. Sol. Energ. Mater. Sol. C 93 (2009) 893*] and [*A. Quatela et al. Microelectronics Reliability 52 (2012) 2487*]

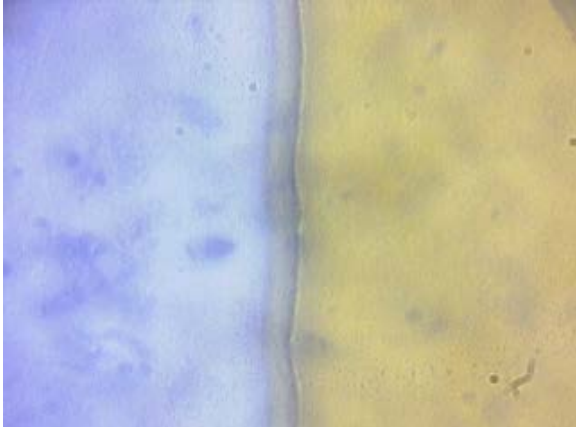
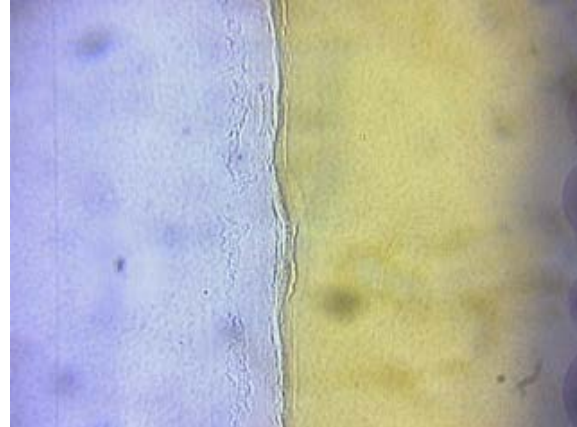
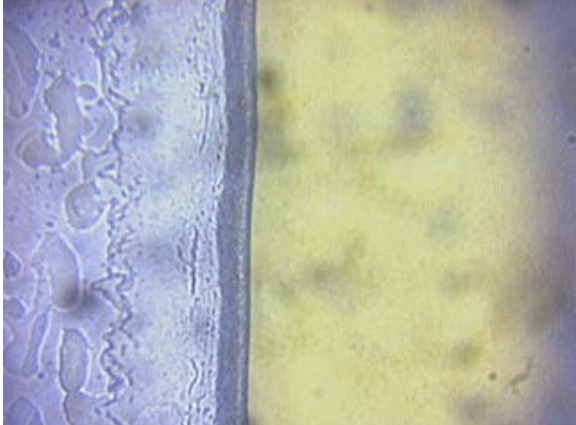
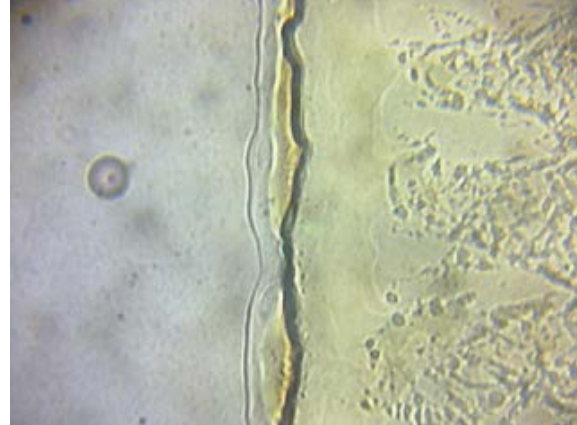
TGL-aged cells: YES, but less pronounced effect

Monitoring dye degradation



- For both cells: No dye degradation in line with previous reports [*Likodimos et al. J. Phys. Chem. C* 113 (2009) 9412]
- For TGL cells: remarkable increase in the signal of the SCN groups in the electrolyte at 2170 cm⁻¹ possibly related to SCN⁻ ligands detached from the dye [*A. Hagfeldt's group*]
after thermal ageing

Sealing integrity?

	MPN	TGL
Fresh	 Micrograph showing a cross-section of a fresh MPN (Micro Permeation Nodule) junction. The left side is stained blue, and the right side is yellow. The interface between the two materials is smooth and well-defined.	 Micrograph showing a cross-section of a fresh TGL (Thin Glass Layer) junction. The left side is stained blue, and the right side is yellow. The interface is smooth and well-defined.
Aged	 Micrograph showing a cross-section of an aged MPN junction. The left side is stained blue, and the right side is yellow. The interface is significantly degraded, showing a porous, irregular structure with many small voids and gaps.	 Micrograph showing a cross-section of an aged TGL junction. The left side is stained blue, and the right side is yellow. The interface is severely degraded, showing a highly porous, irregular structure with many small voids and gaps.